Responses to editor's and referees' comments

Comments to the Author:
Dear authors,

I am glad to accept the paper for publication in ACP. Congratulations! Prior to publication, this paper still need some technical corrections and copy editing as detailed in the referees' comments.

A copy-editing is mandatory and will be done automatically by Copernicus. I will check with the publisher if this service will meet the referee's request.

Sincerely,
Hang Su

Response: Thank you very much for handling our manuscript. We have made technical corrections required by the referee #2. We have also tried to correct the grammatical errors and typos we found. We hope any other language and technical errors will be removed during the Copernicus copy-editing. We provide our point-by-point responses to referees' comments below and include the revised manuscript with track changes.

Anonymous Referee #1
I have reviewed the responses to the first round of reviewer comments. Though the authors made a good-faith effort to address all the reviewer comments, there are still many grammatical errors in the manuscript. This paper will need to be copy edited prior to publication. I'm not sure if this is something that ACP does, so I was not sure whether I should choose "accept subject to technical corrections" or "accept subject to minor revisions".

Response: Thank you for reviewing our manuscript and responses. We have read the manuscript again, and found and corrected some grammatical errors and typos. The manuscript will be copy-edited by Copernicus Publications prior to publication. We hope that all remaining language and technical errors, if any, will be removed during the copy-editing.

Anonymous Referee #2
The authors have made substantial improvements for the revised manuscript and solved most of my concerns. However, there are still some minor errors, which need to be corrected/clarified before the manuscript can be accepted.

1. Page 2, Lines 12: It is vague to say "….from North India, etc". This needs to be clearly demonstrated.

Response: Thank you for your comments. We have changed "from North India, etc" to "from North India, North Pakistan, and Nepal".

2. Page 2, Line 24: Again, there is a typo here, change "+40 (+/-0.2) W/m2" to "+0.4+/-0.2 W/m2".

Response: Yes, this is a typo. It has been corrected as "0.40 ±0.20 W m^{-2}".

3. Figure 7: The figure misses labels of “(a)” and “(b)”.

Response: The labels have been added.

4. Caption of Fig. 9: This should be changed to “Fig. 9. Plots show the …..”

Response: The caption has been simplified as “Fig. 9 The 350 hPa potential vorticity fields at three time-points during 23-24 May 2012 and back trajectories of air masses arriving at 500 m (a,c,e) and 1500 m (b,d,f) above the ground of NMC (red star) during 25-26 May 2012”.

5. Figure 12: There is inconsistent in (c) and (d) between the caption and labels in the Figure. Please make the correction. Also, is the font of “b” in the label larger than the other three? If so, a suggestion here is to make them the same font size.

Response: Corrected. The time periods given in Figs. 12(c) and 12(d) were wrong and have been corrected. The labels “a, b, c, and d” have the same font size.

First simultaneous measurements of peroxyacetyl nitrate (PAN) and ozone at Nam Co in the central Tibetan Plateau: impacts from the PBL evolution and transport processes

Xiaobin Xu[1], Hualong Zhang[1,*], Weili Lin[1,2,], Ying Wang[1], Wanyun Xu[1], and Shihui Jia[1,***]**

[1]{State Key Laboratory of Severe Weather & Key Laboratory for Atmospheric Chemistry of China Meteorological Administration, Chinese Academy of Meteorological Sciences, Beijing, China}

[2]{Meteorological Observation Center, China Meteorological Administration, Beijing, China}

[*]{now at : Guangdong Meteorological Observatory, Guangzhou, Guangdong, China}

[**]{now at: College of Life and Environmental Sciences, Minzu University of China, Beijing, China}

[***]{now at: School of Environment and Energy, South China University of Technology, Guangzhou, Guangdong, China}

Correspondence to: Xiaobin Xu (xiaobin_xu@189.cn)

Abstract

Both peroxyacetyl nitrate (PAN) and ozone (O_3) are key photochemical products in the atmosphere. Most of the previous in-situ observations of both gases have been made in polluted regions and at low altitude sites. Here we present first simultaneous measurements of PAN and O_3 at Nam Co (NMC, 90°57′E, 30°46′N, 4745 m a.s.l.), a remote site in the central Tibetan Plateau (TP). The observations were made during summer periods in 2011 and 2012. The PAN levels averaged 0.36 ppb (range: 0.11-0.76 ppb) and 0.44 ppb (range: 0.21-0.99 ppb) during 17-24 August 2011 and 15 May to 13 July 2012, respectively. The O_3 level varied from 27.9 ppb to 96.4 ppb, with an average of 60.0 ppb. Profound diurnal cycles of PAN and O_3 were observed, with minimum values around 5:00 LT, steep rises in the early morning,

and broader platforms of high values during 9:00-20:00 LT. The evolution of planetary boundary layer (PBL) played a key role in shaping the diurnal patterns of both gases, particularly the rapid increases of PAN and O_3 in the early morning. Air entrainment from the free troposphere into the PBL seemed to cause the early morning increase and be a key factor of sustaining the daytime high concentrations of both gases. The days with higher daytime PBL (about 3 km) showed stronger diurnal variations of both gases and were mainly distributed in the drier pre-monsoon period, while those with shallower daytime PBL (about 2 km) showed minor diurnal variations and were mainly distributed in the humid monsoon period. Episodes of higher PAN levels were occasionally observed at NMC. These PAN episodes were caused either by rapid downward transport of air masses from the middle/upper troposphere or by long-range transport of PAN plumes from North India, North Pakistan, and Nepal~~ete~~. The maximum PAN level in the downward transport cases ranged from 0.5 ppb to 0.7 ppb. In the long-range transport case, the PAN level varied in the range of 0.3-1.0 ppb, with an average of 0.6 ppb. This long-range transport process influenced most of the western and central TP region for about a week in early June 2012. Our results suggest that polluted air masses from South Asia can significantly enhance the PAN level over the TP. As PAN act as a reservoir of NO_x, the impacts of pollution transport from South Asia on tropospheric photochemistry over the TP region deserve further studies.

1 Introduction

Peroxyacetyl nitrate (PAN) and ozone (O_3) are important species in the troposphere. They are toxic for human and vegetation. Tropospheric O_3 contributes significantly to global warming with a radiative forcing of ~~+~~0.40 ~~(~~±0.20~~)~~ W~~/~~ m^{-2} (Myhre et al., 2013). Tropospheric O_3 originates mainly from photochemical reactions within the troposphere and to a lesser extent from the stratosphere (Lelieveld and Dentener, 2000), while PAN in the troposphere is nearly exclusively formed in the oxidation of volatile organic compounds (VOCs) in the presence of nitrogen oxides (NO_x) (Fischer et al., 2014). PAN is produced in the association reaction between peroxyacetyl radical ($CH_3C(O)O_2$, PA) and nitrogen dioxide (NO_2). As one of the key radicals, PA is produced by oxidation of a number of VOCs (Roberts, 2007; LaFranchi et al., 2009; Fischer et al., 2014). Since both VOCs and NO_x are largely emitted by anthropogenic sources, PAN is primarily produced in and downwind of industrial and populated areas. In additional to anthropogenic sources, PAN is also formed in biomass

burning plumes (Tereszchuk et al., 2013; Fischer et al., 2014; Zhu et al., 2015). With different lifetimes at different temperatures (Cox and Roffey, 1977), PAN is instable under warm conditions, but stays longer in colder environment. Due to this ~~characteristis~~ characteristic PAN is ubiquitous in the middle to upper troposphere (Singh, 1987; Talbot et al., 1999; Russo et al., 2003; Kramer et al., 2015) and can be transported in higher altitudes in a global scale. PAN can decompose and release NO_2 when it reaches warm environment, becoming one of the key sources of NO_x in remote areas. This makes PAN an important reservoir of NO_2. Inter-comparisons among models and between model and observation show~~ed~~ very large PAN differences in many regions of the atmosphere (Thakur et al., 1999; Sudo et al., 2002; von Kuhlmann et al., 2003; Singh et al., 2007), but confirm~~ed~~ the important role of PAN in sustaining O_3 production over remote regions (Hudman et al., 2004; Zhang et al., 2008). Since tropospheric O_3 and OH are principally controlled by the abundance of NO_x, decomposition of PAN ~~would~~ may have great implications for the budget of these key atmospheric oxidants. It has been indicated that regional increase of O_3 can be attributed to an intercontinental and even global transport of PAN (Hudman et al., 2004; Fischer et al., 2011) and most of the conveying paths are in the free troposphere, driving PAN plumes travelling to remote areas (Roiger et al., 2011; Pandey Deolal et al., 2013). Thus, a considerable amount of PAN has been detected in remote areas with sparse anthropogenic emission (Zanis, 2007).

Up to now the main methods to directly obtain the PAN concentration are ground-based and aircraft observations. Although PAN has been measured in a great deal of campaigns ~~during past~~since decades, the observational data of PAN have been very inhomogeneously distributed over the world, with most of them being from North America, West Europe, and Pacific region (Fischer et al., 2014). PAN measurements are extremely lacking in many areas over the Eurasian continent, northeastern African, Oceanic regions, the Indian Ocean, and the Tibetan Plateau (TP) region.

The TP region covers an area of about 2,500,000 km^2, with an average elevation of about 4000 m above sea level. The world's highest plateau acts as a heat source in summer, heating the air above and prompting its ascending motion (Yeh et al., 1957). In addition to the thermal effect, the South Asian monsoon also exerts a convergence effect driving the ascending motion (Chen et al., 2012). Accompanied by the ascending motion, water vapor and air pollutants emitted or formed in the boundary layer can be rapidly transported to the upper troposphere and lower stratosphere (UTLS) (Dessler and Sherwood, 2004; Gettelman and

Kinnison, 2004, Fu et al., 2006; Lelieveld et al., 2007; Law et al., 2010). Convective transport over the TP and surrounding areas can be clearly tracked by satellite observations of some longer-lived species, such as CO (Park et al., 2007, 2009), PAN (Ungermann et al., 2016), CH_4 (Xiong et al., 2009) and HCN (Randel et al., 2010). Elevated concentrations of some relatively short-lived anthropogenic pollutants in the UTLS region are also reported (Park et al., 2008, Tian et al., 2008; Gu et al., 2016). Such rapid, upward transport of pollutants and water vapor may have great implications on atmospheric composition and climate of regional and global scales. Efforts have been made to understand the impacts of upward transport of air masses over the TP, among which is the potential relationship with the ozone valley over the TP reported by Zhou et al. (1995).

The TP region is very sparsely populated with nearly no industrial emissions of pollutants. Although the TP has been nearly unpolluted, the high altitude and the correspondingly intensified UV radiation make it an interesting region for studies of photochemical products, such as O_3 and PAN. However, there have been only sparse reports of measurements of O_3 and related species from the TP mainly due to the poor accessibility and logistic difficulties of this vast region. So far, most of the published measurements of O_3 and its precursors over the TP have been from sites at the edges of the TP (Ma et al., 2002a, 2002b; Ding and Wang, 2006; Wang et al., 2006; Zhu et al., 2006; Cristofanelli et al., 2010; Xue et al., 2011; Zheng et al., 2011; Ma et al., 2014; Wang et al., 2015b; Xu et al., 2016, 2018). Only three publications present measurements of O_3 and related species from sites in the central TP, with one reporting data from urban observations (Ran et al., 2014) and two showing results from remote sites (Lin et al., 2015; Yin et al., 2017).

Observational data of PAN from the TP are extremely lacking. The only field observation of ambient PAN in the TP was made by Xue et al. (2011), who measured PAN and other reactive species at Mt. Waliguan, a global atmosphere watch (GAW) station located at the northeast edge of the TP. The average level of PAN was 0.44 ($\pm$0.14) ppb for a two-week period in summer 2006. This observation offers a preliminary detection of ambient PAN over the northeast TP. So far, there has been no published in-situ measurement of PAN from the central TP. In addition to the traditional observation methods, remote sensing techniques can also be applied to acquire the global PAN distribution from satellites (Remedios et al., 2007; Moore and Remedios, 2010; Wiegele et al., 2012; Tereszchuk et al., 2013; Fadnavis et al.,

2014). However, the PAN data retrieved from satellite observations need further validations and do not cover the lower and middle troposphere.

Here we present the first simultaneous measurements of PAN and O_3 at a site in the central TP. We study the diurnal variations of observed concentrations and the links to the evolution of planetary boundary layer (PBL). We also investigate the vertical and horizontal transport and discuss the implications of our measurements.

2 Observations

2.1 Site

The observations of PAN and other species were made from 11 July to 31 August 2011 and from 15 May to 13 July 2012 at the Nam Co Comprehensive Observation and Research Station, Chinese Academy of Sciences (CAS) (NMC, 90 °57′E, 30 °46′N, 4730 m a.s.l.). West and north of the NMC site is the Nam Co Lake, with the nearest distance to the lake being about 1.5 km. The Nyainqentanglha ~~mountains~~ Mountains (about 5000-6800 m a.s.l.) stand south and east of the site, with the nearest mountain ridge being more than 20 km distant from the site. The TP region has a population density of less than 2 person/km^2 (http://sedac.ciesin.columbia. edu/gpw/, last access: 1 April 2018). The largest city of Tibet, Lhasa, is about 120 km south of the NMC site, far beyond the continuous ridges of the Nyainqentanglha Mountains. The nearest population center, Dangxiong ~~township~~Township is located about 35 km southeast of the NMC site. The direct transport of air pollutants from Lhasa and Dangxiong is limited due to the blocking of the high mountain ridges. There is a road about 1.3 km southeast of the NMC site, connecting the tourism site of the Nam Co Lake to Dangxiong and the No. 109 National Road. More details about NMC and its surrounding can be found in literature (Ma et al., 2011; Lin et al., 2015; Yin et al. 2017).

2.2 Instruments and data correction

Ambient PAN was observed using a PAN analyzer (Meteorologie Consult GmbH, Germany), which consists of an automated gas chromatograph (GC) equipped with an electron capture detector (ECD) and a calibration unit. The equipment is the same one as used in previous observations in Beijing (Zhang et al., 2014) and elsewhere (e.g., Zellweger et al., 2000; Zhang et al., 2009a), with identical setup details depicted in Zhang et al. (2014). The GC with a pre-column and a main column was optimized by the factory for the separation of PAN and CCl_4

at 15℃ within 10 min. Purified nitrogen (>99.999%, Chengweixin Gases, Beijing, China) was used as carrier gas. A cartridge with $CuSO_4$ $5H_2O$ was used to humidify the carrier gas before entering the GC columns. This can reduce the effects of varying humidity on the measurements (Flocke et al., 2005). Back-flushing was applied to the pre-column to prevent contamination and shorten analysis time. An NO reference gas (4.5 ppm, Huayuan Gases, Beijing, China) in nitrogen was introduced into the calibration unit, ~~and~~ where it reacts with excess acetone vapor under the UV irradiation to yield concentrated PAN. Prior to each campaign the NO reference gas was verified using an NO standard (Air Liquide America Specialty Gases LLC, USA) traceable to the National Institute of Standards and Technology (NIST) reference material. Under similar conditions, the PAN yield was found to be 92%±3% (Volz-Thomas et al., 2002). A continuous, stable flow of known PAN concentration was produced by subsequent dynamic dilution with purified ambient air and supplied to the PAN-GC for calibration. The lower detection limit was 50 ppt. Zellweger et al. (2000) achieved an overall uncertainty of ±3% under their conditions.

Surface O_3 was simultaneously observed using an O_3 analyzer (TE 49C, Thermo Environmental Instruments, Inc., USA). The O_3 analyzer has a lower detection limit 1.0 ppb and precision of ±1.0 ppb. Before and after each campaign the analyzer was calibrated using an O_3 calibrator (TE 49C PS) traceable to the Standard Reference Photometer (SRP) maintained by WMO World Calibration Centre in EMPA, Switzerland (Zellweger et al., 2009). All instruments were housed in a simply constructed one-storey building, located 0.15 km southeast of the station's main building. Ambient air was introduced through Teflon tubing (O.D. 1/4" and 2-3 m) to the PAN and O_3 analyzer at the flowrate of 2 l/min and 6 l/min, respectively. Meteorological data were collected using automatic meteorological station systems installed at different levels on a tower near the observation building.

Although measurements of PAN have been made previously at some high-altitude sites in other areas using methods similar to ours (Ford et al., 2002; Fischer et al., 2010; Xue et al., 2011; Pandey Deolal et al., 2013), this is the first report of using the GC-ECD instrument for PAN measurement under the conditions of a high-altitude site over 4700 m a.s.l. To track the performance of the PAN analyzer, frequent calibrations were made during the campaigns (e.g., on 9 and 10 July, 7, 9, 12, 14, 17, and 23 August 2011, and on 15, 16, 28 May, 6, 13, 20, 22, 27 June, 4, 12, and 13 July 2012) except the period from 16 July to 5 August 2011, where no carrier gas was available for the PAN observation due to a leakage. During the observation

period in 2011, the instrument performance was somewhat instable, probably affected by the extreme ambient conditions at the site. The variation of environment temperature is suspected to have made it hard to keep the ECD inner temperature constant. This resulted in abrupt fluctuations in the 10-min chromatographic PAN signals sometimes during the measurement period in 2011. The instable performance of ECD caused varying detection sensitivity. Normally, we convert PAN signals of air samples to concentration data based on ratios of signals to theoretical PAN concentration of the standard gas produced during the calibrations. However, the jumping sensitivity made it improper to obtain PAN concentrations using the normal method. Thus, we applied an indirect calibration method. Our GC-ECD instrument was optimized for the separation and detection of both PAN and CCl_4. Therefore, it was possible to indirectly calculate the PAN concentrations, i.e., by using the ratios of the PAN to CCl_4 signal. Details about the indirect calibration are given in the supplement.

Although the indirect calibration is a viable way to obtain PAN concentrations, the uncertainty of final data could be larger than the direct calibration primarily due to the two assumptions mentioned in the supplement and some technical problems with the observation system. We are more confident of the data from 17 to 24 August 2011. During this period, the instruments performed well and the two calibrations in this period gave similar sensitivities. In view of this, we report and analyze in this paper mainly data from 17 to 24 August 2011, together with those obtained from 15 May to 13 July 2012, where our instruments performed well.

2.3 Meteorological data and analysis

Local meteorological variables, including temperature, relative humidity, 3-dimensional winds, etc., were observed by corresponding sensors installed at 2 m, 10 m, and 20 m of the meteorological tower at the NMC station. The National Centers for Environmental Prediction (NCEP) reanalysis data, together with the local meteorological data, are used in this paper to facilitate the interpretation of our PAN and O_3 measurements. Global Data Assimilation System (GDAS, 3 hourly, $1° \times 1°$ in longitude and latitude, and 26 pressure levels, http://ready.arl.noaa.gov/gdas1.php, last access: 1 April 2018) data were obtained from National Oceanic and Atmospheric Administration (NOAA) Air Resources Laboratory (ARL). The GDAS data ~~were~~ are used as input to the Hybrid Single-Particle Lagrangian Integrated Trajectory (HYSPLIT) model (V4.9) for simulating backward air trajectories ending at 500 m

and 1500 m above the NMC site. The HYSPLIT model is developed by NOAA/ARL (Draxler and Hess, 1997). In addition, NCEP FNL(final) Operational Global Analysis data (6 hourly, 1° × 1° in longitude and latitude, and 26 pressure levels, http://rda.ucar.edu/datasets/ds083.2/#!description, last access: 1 April 2018) were acquired from National Center for Atmospheric Research (NCAR). These data ~~were~~ are used to obtain meteorological fields for analyzing weather patterns and air circulations over the TP.

3 Results and discussion

3.1 Surface concentrations of PAN and O_3

The PAN level averaged 0.36 ppb in the period of 16-25 August 2011, ranging from 0.11 ppb to 0.76 ppb. A clear increasing trend is found in the time series of PAN data in this period. The origin of increasing PAN in such period will be discussed in section 3.4. In 2012, the effective observation covered nearly two months (from 15 May to 13 July), long enough to obtain the PAN levels under different atmospheric conditions during the South Asian Monsoon period. The observed PAN in this period varied from 0.16 ppb to 0.99 ppb, with an average of 0.44 ppb. This result is close to the PAN levels observed in summer 2006 at Waliguan (WLG), a remote site at the northeastern edge of the TP (Xue et al., 2011). The O_3 concentration varied from 27.9 ppb to 96.4 ppb, with an average of 60.0 ppb, nearly identical to the average O_3 level at WLG. There were little day-to-day and diurnal variations when the PAN and O_3 measurements from WLG were not impacted by relatively polluted airmasses from the eastern sector (Xue et al., 2011). In contrast, our PAN and O_3 measurements from NMC show profound variations. The reasons of the variations, particularly the diurnal variations, should be investigated.

It is noteworthy that the NMC site is about 20 km distant from the Nyainqentanglha Mountains. Permanent snow cover exits on the mountains. Experiments by Ford et al. (2002) indicated that snowpack at Summit, Greenland emitted PAN. Snowpack may also emit NOx, HONO, etc., and indirectly influence the O_3 formation over Summit (Huang et al., 2017). However, the snowpack influence may only play a minor role in the budget of PAN and O_3. For example, ambient PAN over the Summit site was dominated by transport instead of snowpack emission though the site is permanently covered with snow (Ford et al., 2002). The annual mean snow line altitude of the Nyainqentanglha Mountains was about 5.8 km a.s.l. in 2013 (Zhang et al., 2016). In summer, the snow line is even higher though snow may exist on

the glaciers extending to lower elevations (Qu et al., 2014). At this time, we cannot exclude the possibility of snowpack influence on our measurements. However, this influence might be very limited because of the large distance between NMC and the snow areas. Therefore, we focus on other factors that may influence the variations of PAN and O_3 at NMC.

3.2 Diurnal cycles of PAN and O_3 and potential impacts from the PBL evolution

The 10-min PAN and O_3 concentrations observed in 2012 were used to obtain the averaged diurnal patterns (Fig. 2). As can be seen in Fig. 2, during night time both PAN and O_3 show a decreasing trend and reach the valley around 5:00 Local Time (LT, here LT=Beijing Time – 2h), demonstrating their steady loss during night. From 5:00 LT to 10:00 LT, both gases can be characterized by rapid increase, with the average levels of PAN and O_3 being lifted over 0.10 ppb and 15.0 ppb, respectively. Subsequently, O_3 increases at a much lower rate before reaching its peak around 16:00 LT and then starts to decline. Unlike O_3, PAN behaves more fluctuating after its peak time (around 12:00 LT), with a larger deviation from the trace of O_3.

It is noteworthy to see the sharp early-morning increase of PAN and O_3 as shown in Fig. 2. If the observed increase of both gases had been caused by photochemical productions, considerable amount of their precursors would be required to fuel the photochemical reactions. However, according to the EDGAR 3.2FT2000 database, anthropogenic emission in TP is extremely low, with emissions of NO_x and CO being respectively no more than 0.1×10^{-12} kg/m^2/s and 1×10^{-12} kg/m^2/s in the surrounding areas (http://themasites.pbl.nl/tridion/en/themasites/edgar/emission_data/edgar_32ft2000/index-2.html, last access: 1 April 2018). Surface NO_x at NMC was below the lower detection limit of the commercial NO_x analyzers like TE42CTL and Eco Physics CLD88p that we deployed there. In addition, the key condition for the photochemistry, i.e., the UV radiation, was not strong enough to drive photochemical reactions in the very early morning (say around 5:00 LT), as the sunrise in that TP area occurs around 6:00 LT in summer. Therefore, it is hypothesized that the main factor driving the rapid PAN and O_3 increase in the early morning was not photochemistry but the mixing process during the PBL evolution. To prove this hypothesis, we display scatter plots in Fig. 3, showing the correlations between the increment of O_3 concentration (ΔO_3) and that of PAN concentration (ΔPAN) for two time periods of the day, and the correlation between the increments of O_3 and temperature (ΔT). Figure 3(a)

represents data from the 5:00-9:00 LT period, when the solar radiation becomes gradually intensive. Figures 3(b) and 3 (c) show data from the 2:00-4:00 LT period, when no solar radiation is available for the local photochemical reactions.

Significant linear correlation between ΔO_3 and ΔPAN is found for both the early morning period (Fig. 3(a)) and the dark period (Fig. 3(b)), with correlation coefficients of 0.745 and 0.711, respectively. Although photochemical reactions, in which both O_3 and PAN are produced, can lead to a ΔO_3-ΔPAN correlation, they cannot occur during the dark period. Therefore, the significant correlation in Fig. 3(b) should be attributed to some meteorological processes instead of photochemical process. Moreover, the ΔO_3-ΔT correlation shown in Fig. 3(c) further indicates that the concentrations of surface O_3 and PAN at the site may be influenced purely by some meteorological processes that change air temperature as well. The net change of O_3 could be positive before dawn, and occurred on those days with simultaneously rising PAN and temperature. The rising temperature could be related to the dry adiabatic heating process during air masses descending. Such a process happens when the PBL is extended, not necessarily driven by solar radiation. Downward transport of PAN and O_3 may accompany such process. Therefore, the PBL evolution might have significantly impacted the diurnal variations of PAN and O_3 at NMC.

3.3 Insight into the PBL evolution

The evolution of PBL plays one of the key roles in the diurnal variations of surface meteorological parameters and air pollutants, and is influenced by the dominating synoptic situation. It has different diurnal patterns under different synoptic situations. Here we take the O_3 enhancement (ΔO_3) in the early morning as an indicator quantity to find out major differences in the evolution of the PBL and some related parameters under different synoptic situations. We select~~ed~~ 30 days from the observation period in 2012 and separat~~ed~~ them into two groups, with Group 1 including 15 days with the greatest ΔO_3 values (High ΔO_3) and Group 2 including 15 days with the smallest ΔO_3 values (Low ΔO_3). For the two groups, average diurnal variations were calculated for PAN, O_3 and some meteorological parameters, i.e., wind speed at 2 m above ground (Ws), U wind speed at 2 m above ground (Us), V wind speed at 2 m (Vs), the ratio between the 2-m and 10-m wind speeds (WSR), the temperature difference between 20 m and 10 m (TD), and water vapor pressure (WVP). The obtained diurnal variations are plotted in Fig. 4.

A stable nocturnal boundary layer (NBL) forms gradually in the night (Stull, 1988). A temperature inversion can occur in the NBL, with the air temperature increasing with height. A nocturnal jet may form over the NBL so that a larger gradient of wind speed may exist in the NBL. Such stratification prevents the air from being vertical mixed in the night and is broken in the early morning. As a result, the concentrations of O_3 and PAN at the ground-level decrease largely in the nighttime because of chemical and physical losses and increase rapidly in the early morning because of the downward mixing of upper-level air containing more O_3 and PAN. This evolution of PBL, however, can be strongly impacted by some systematic processes so that the day-night differences of PBL are weakened or even disappear. We believe that the two groups of data presented in Fig. 4 represent approximately two circumstances of the PBL evolution, with the High-ΔO_3 group being less or not impacted and the Low-ΔO_3 group being strongly impacted by the systematic processes.

As can be seen in Fig. 4, the Low-ΔO_3 group showed much smaller diurnal variations of PAN, O_3, Ws, WVP, and WSR, suggesting a weak day-night cycle of the PBL. Compared with the values in the Low-ΔO_3 group, the nighttime values of PAN, O_3, Ws, and WSR in the High-ΔO_3 group were much lower, and that of TD much higher. Lower WSR and higher TD in the night indicate a more stable NBL, which explains the lower PAN and O_3 levels as discussed above. After dawn the values of PAN, O_3, Ws, WSR, and TD in the High-ΔO_3 group changed rapidly back to their daytime levels, indicating the break of the stable NBL. It is noteworthy that there were virtually no or only minor differences in the daytime values of PAN, Ws, WSR, and TD between the two groups. The daytime O_3 in the High-ΔO_3 group reached significantly higher levels than that in the Low-ΔO_3 group. Moreover, the WVP value in the High-ΔO_3 group was lower than that in the Low-ΔO_3 group during the entire day. These phenomena imply that the High-ΔO_3 group is related to drier days and PBL conditions favoring the increase of surface O_3 during daytime (e.g., through downward mixing) and destruction during nighttime, while the Low-ΔO_3 group is related to more humid days and PBL conditions that inhibit the variation of surface O_3.

The PBL evolution was investigated in previous field experiments in the TP. Li et al. (2011) found that there were some differences in the diurnal evolution of the PBL structure between dry and rainy seasons. In the dry season, namely the pre-monsoon period, a shallow but strong inversion layer could be clearly observed at night. The occurrence of the inversion layer is high in the pre-monsoon period, simply because the PBL structure is primarily driven by

sensible heat (Ma et al., 2005). The outflow of sensible heat at night is massive according to thermal analysis. In the rainy season, a shallower but more persistent wet convection evolves, forcing efficient exchange of quantities and also comparably smaller gradients of meteorological elements. The daytime PBL height can reach 4-5 km above the ground in the dry pre-monsoon period, while it is usually about 1-2 km above the ground in the wet monsoon period (Li et al., 2011; Chen et al., 2013). In our case, prevailing monsoonal features are perceivable in meteorological measurements associated with the Low-ΔO_3 group, such as weaker westerly wind (U wind, Fig. 4(g)), stronger southerly wind (V wind, Fig. 4(h)) and higher WVP (Fig. 4(d)). Unlike the dry season, the convection intensity in the wet season had a much smaller diurnal variation, as suggested by the smaller day-night differences of WSR and TD. Thus, in the wet season, downward transport of PAN and O_3 during nighttime might have been much more effective than that in the dry season. This can explain the observed nighttime differences in the PAN and O_3 concentrations between the Low-ΔO_3 and High-ΔO_3 groups (Figs. 4(a) and 4(b)).

To know more details about the two groups of days discussed above, the distribution of the Group 1 and Group 2 days, together with parameters including the PBL height, precipitable water of entire atmosphere (PWAT), WVP, and the PAN and O_3 concentrations are shown in Fig. 5. The PBL height and PWAT values are obtained from the NCEP FNL reanalysis data. It can be seen that the surface measured WVP is in good accordance with the PWAT in trend. The whole observation period in 2012 can be divided into dry period and wet period. The transition between the wet and dry periods can be easily identified based on the changes of the PBL height, and the PWAT and WVP values. It can also be seen in the variation of the daily rainfall at NMC (Fig. S1). We can see a sudden seasonal change in the middle of June, when the depth of PBL was suppressed after 16 June 2012 (marked with green bar in Fig. 5) and the water amount became more abundant, suggesting the onset of the South Asian monsoon. The distributions of the two groups of days are labeled on Fig. 5(a). Although there are some irregular cases, the High-ΔO_3 days (Group 1) are mostly distributed in the dry period and the Low-ΔO_3 days (Group 2) in the wet period. This supports our analysis in previous paragraph. The time series of the PBL height indicates that the daily maximum PBL heights in the dry period were much higher than those in the wet period, with only a few exceptions. Such phenomenon agrees with the observational results from Naqu, about 230 km northeast of NMC (Li et al., 2011). The nocturnal PBL height in the dry period could be extremely low

(frequently lower than 200 m). This explains the lower nighttime PAN and O_3 values in the High-ΔO_3 group (Fig. 4).

In the pre-monsoon there may be episodes with monsoon features. An example of this is the period of a few days around early June 2012, where the PBL height was considerably suppressed, and the PWAT, WVP as well as the concentrations of PAN and O_3 were significantly enhanced (Fig. 5). In this relatively humid episode, the nighttime concentrations of PAN and O_3 were largely elevated, which may be attributable to the PBL structure and airmasses transported from the polluted region (see section 3.5).

In conclusion, the South Asian monsoon brings not only more water vapor over the central Tibet area but also effectively drives the PBL evolution, which plays an important role in shaping the diurnal patterns of PAN and O_3 at the NMC site.

3.4 O_3 and PAN abundance under the impact from UTLS

It is noticeable in Fig. 4 that the levels of daytime O_3 were considerably different between the two groups, while those of daytime PAN were close to each other. In the average diurnal curves of O_3 and PAN (Fig. 4), the highest hourly O_3 levels for Groups 1 and 2 were 69.7±2.4 ppb and 59.0±2.5 ppb, and the highest hourly PAN levels were 0.48±0.02 ppb and 0.49±0.05 ppb, respectively. Observations at WLG showed that air masses from higher altitudes (i.e., UTLS) contained higher O_3 and lower PAN (Xue et al., 2011). As shown in Fig. 5, the daytime PBL in Group 1 could reach much higher altitudes than that in Group 2, indicating a higher probability of downward mixing of O_3–richer air from the middle and upper troposphere on the days in Group 1. Therefore, the higher daytime O_3 value for Group 1 is qualitatively consistent with the observational results from WLG (Xue et al., 2011). Only negligible distinction of daytime PAN was found between the two groups, implying that on average, air masses from higher altitudes did not cause lower or higher daytime PAN.

Surface levels of air pollutants at any sites depend mainly on local chemistry, transport and deposition. Since the TP is a pristine and high-altitude region with litte emissions of O_3 and PAN precursors, local chemistry cannot cause large day-to-day variations of these species, as shown in Ma et al. (2002b). Therefore, a large fluctuation in the daytime levels indicates usually a substantial change of transport contribution, particularly vertical transport. In general, the O_3 level increases from the ground to the UTLS. This is also true over the TP and its surrounding areas, as shown by Worden et al. (2009). In some cases, air masses in the

UTLS with O_3 close to or higher than 100 ppb can be downward transported to near ground, causing high surface O_3 events. Such cases have been often observed at high altitude sites (Ding and Wang, 2006; Wang et al., 2006; Helmig et al., 2007; Cristofanelli et al., 2010; Lefohn et al., 2012; Ma et al., 2014; Huang et al., 2017; Xu et al., 2018) and occasionally also at some low altitude sites (e.g., Lefohn et al., 2012). Thus, surface O_3 concentration observed at sites in the TP region can sometimes be used as an indicator of air masses from the higher altitudes and also reflects the depth of developed PBL. Observations at Summit (3212 m a.s.l), Greenland showed that air masses from the UTLS always accompanied with high ozone and low water vapor events (Helmig et al., 2007; Huang et al., 2017). As the WVP profile over the TP shows a clear decrease with height (Chen et al., 2013), air masses from high altitudes over the TP can also be indicated by lower WVP.

To gain more insight in air masses from upper origins, we attempt to differentiate air masses originated in the upper troposphere from other air masses. Following the grouping of days in section 3.3, scatter plots of PAN-O_3, WVP-O_3, and WVP-PAN are shown in Fig. 6 for the two groups. The data points within the red rectangle in Fig. 6(c) are measurements associated with higher O_3 levels and lower WVP. We consider these as measurements with significant features of middle/upper tropospheric air since they are above the highest average hourly O_3 level (69.7 ppb) shown in Fig. 4(b) and associated with WVP < 500 Pa. Fig. 6(b) displays a good positive PAN-O_3 correlation for Group 2, which is consistent with simultaneous photochemical production of both secondary pollutants. However, the dataset from Group 1 shows a much weaker PAN-O_3 correlation (Fig. 6(a)), indicating a weaker relationship between PAN and O_3 in Group 1. Nearly no correlation between PAN and WVP is found (Fig. 6(e)). At present, the actual causes of the poor PAN-O_3 and PAN-WVP correlations are unknown. However, it is reasonable to believe that on the days in Group 1, the observed O_3 level was more influenced by air masses from the UTLS, where the O_3 level is higher and the PAN level lower than at the surface (Worden et al., 2009; Moore and Remedios, 2010). In addition, it is suspected that the horizontal variability of PAN was larger than that of O_3 during our observations.

Figure 6 does not allow for an estimate of PAN abundance in upper levels. However, we can make use of some cases with deep convection and apparent downward transport activities in the dry period. Here we try to deduce the origins of air masses in two cases and roughly estimate the PAN concentrations associated with air masses from upper levels. The two cases

chosen for analysis are 25 May 2012 and 24 August 2011. Figure 7 displays the vertical velocity (omega) fields and horizontal wind vectors at different times and air pressure levels, with the two cases being labeled with black rectangles (termed as Case 1 and Case 2). Positive and negative omega values indicate descending and ascending, respectively. Both cases were from dry periods, when the PBL could reach higher heights and favor the entrainment of upper air-masses.

Figure 7(a) shows that positive omega dominated the PBL from early 25 May 2012 to early 26 May 2012 (Case 1), with the range of higher omega (>0.1 hPa/s) extending from surface to 350 hPa, and a distinct valley of specific humidity line of 2g/kg, indicating a strong downward transport. In response to this downward transport, PAN and O_3 were both elevated to higher levels and WVP decreased to about 200 Pa (Fig. 5). A similar case occurred during 22-23 August 2011 (Case 2), as shown in Fig. 7(b). On 22 August, the height with descending air extended from the ground up to 300 hPa and lasted all day long, with very high intensity (omega > 0.3 hPa/s). For better understanding of Case 2, we display in Fig. 8 the time series of O_3, PAN, and related meteorological parameters during 16-25 August 2011. The O_3 and PAN levels increased rapidly on 22 August 2011, as indicated by the arrow in Fig. 8(b). In parallel with the increases of O_3 and PAN levels, relative humidity and wind vector changed rapidly, with the former dropping dramatically from 80% to about 30% and the later turning from southerly to northerly. Similar rapid variations were also observed partly during 23-24 August 2011, corresponding to the subsiding of dry air masses (Fig. 7(b)).

It is noticeable that the daytime levels of O_3 and PAN did not show much distinction among the days from 22 to 24 August 2011. This suggests that the air masses arriving at our site during the period might originate from similar height and area. To prove this, we calculated backward trajectories with endpoints at 500 m and 1500 m above the ground of the NMC site. Some of the trajectories for the two selected cases, 25 May 2012 (Case 1) and 22 August 2011 (Case 2), are plotted in Figs. 9 and 10, respectively, overlaying on the 350 hPa potential vorticity (PV) fields at three time points during 23-24 May 2012 (for Case 1) and during 20-22 August 2011 (for Case 2), respectively. Similar plots with the same trajectories and 250 hPa PV fields are shown in Figs. S2 and S3 for Case 1 and Case 2, respectively. In both cases stratospheric intrusions occurred as indicated by the higher PV values (>2). In Case 1 (Figs. 9 and S2) higher PV covered the zone from 30 ℕ to beyond 50 ℕ. In Case 2 (Figs. 10 and S3) higher PV extended from about 40 ℕ to beyond 50 ℕ. In both cases air masses arriving at the

NMC site originated from or travelled through the zones between 350 hPa and 250 hPa that were obviously impacted by stratospheric intrusions. Therefore, the PAN and O_3 measurements in both cases were influenced by air masses from the UTLS. In addition to the transport feature, the elevated O_3 and decreased water vapour amount in surface air also indicate impacts of high–level air masses. For Case 1 and Case 2, the PAN level was elevated respectively up to 0.52 ppb and 0.72 ppb, which can be regarded as the maximum PAN levels observed under the impact from UTLS.

3.5 A PAN episode driven by South Asian monsoon

In warm environment, PAN is short-lived. Below 7 km, thermal decomposition is the main loss process of PAN (Talukdar, 1995). Thus, although polluted air masses from south of the Himalayas can be transported to the TP along the monsoon stream, PAN in the air masses may experience significant loss during the travelling. Cox and Roffey (1977) estimated the lifetime of PAN at 25 ℃ to be about 2.7 h and 0.7 h for urban and rural daytime conditions, respectively, and that at 15 ℃ a factor of four longer. During our observations in summer 2012, surface air temperature at NMC varied from -0.5 ℃ to 19.4 ℃, with an average of 8.4 ℃. Thermal decomposition should be much slower under such temperature condition and only important during warmer daytime periods. However, thermal decomposition might still have removed a significant fraction of PAN during the long-range transport, particular over the warm low-elevation areas. The level of PAN observed at our site was the remaining PAN in the air masses, which should be significantly lower than that in the formation area. Nevertheless, PAN episodes were observed under certain meteorological conditions. One of such episodes occurred in early June 2012. As can be seen in Fig. 5, the PAN level humped during 1-6 June 2012. The maximum PAN level reached 1.0 ppb, and the diurnal minima on these days were even higher than the diurnal maxima on many of other observation days. The origin of the high PAN levels deserves an investigation.

Data in Fig. 5 indicate that the monsoon flow prevailed persistently after the middle of June 2012, and there were also some features of monsoon impact during 1-6 June 2012 when the PAN level was increased to near 1 ppb. After this abrupt rising, PAN dropped down to much lower level, suggesting a substantial change in air mass. To understand this phenomenon, we calculated average fields of wind, relative humidity, and omega at sigma=0.995 for the periods 30-31 May using the FNL reanalysis data. During 30-31 May 2012, the major part of Indian subcontinent was controlled by an anticyclone system and a large convergence zone

formed over the central TP (see Fig. S4). The NMC site was within this convergence zone and obviously influenced by airflow from North India. Figure 11 shows the average wind fields for 12:00 (UTC) of 4, 5, 7 and 8 June 2012. These wind fields give a clue to the origin of high level of PAN observed during 1-6 June 2012. As indicated by the wind fields in Figs. 11 and S4, after 30 May the NMC site was influenced by westerly and southwesterly winds, which could transport air masses from South Asia to the NMC site. After this period, the site was influenced by significantly different air masses. For example, the average wind fields shown in Figs. 11c and 11d indicate that after 7 June 2012, strong southerly and southeasterly winds developed over East India and Southeast Nepal, and southerly wind prevailed over the area surrounding NMC, which promoted the transport of air masses from the Bay of Bengal. Although most of the central and western TP was within the convergence zone, NMC and its surrounding were outside of its direct impact. Such change in air masses arriving NMC inevitably caused substantial differences in photochemistry. Northern India suffers photochemical pollution, as indicated by observations of high level of surface O_3 (Ghude et al., 2008) and tropospheric O_3 (Fishman et al., 2003). Emission inventories (Ohara et al., 2007; Zhang et al., 2009b) indicate that North India is one of the Asian emission centers for pollutants including NO_x and VOCs. In additional to anthropogenic sources, biomass burning is also an important source for PAN, and some of biomass burning plumes can penetrate the boundary layer and cause PAN formation over a large scale (Tereszchuk et al., 2013; Fischer et al., 2014; Zhu et al., 2015). Figure S5 shows tropospheric NO_2 and HCHO columns, together with maps of fire spots for 1-3 and 4-6 June 2012. As can be seen in this figure, NO_2 and HCHO in the troposphere over North India and North Pakistan were highly abundant during both periods. However, the NO_2 and HCHO levels were obviously higher during 1-3 June than during 4-6 June. The differences in NO_2 and HCHO levels might have been caused by open biomass burning since much more fire spots were observed during 1-3 June than during 4-6 June (see Figs. S5(e) and S5(f)). The high tropospheric NO_2 and HCHO columns suggest the presence of high concentrations of NO_x and VOCs, which may lead to rapid formation of O_3 and PAN under the summer conditions over the South Asian region. Since this region borders on the TP, it is likely that the PAN episode observed at our site during 1-6 June 2012 was mainly caused by long-range transport of plumes with high PAN and its precursors from South Asia.

To further support the above view, we made calculations of backward air trajectories. The results are presented in Fig. 12. The 5-day trajectories were calculated for endpoints at 500 m

and 1000 m above ground for 1-6 June and ~~7~~6-10 June 2012, respectively. Obviously, air trajectories arriving NMC during 1-6 June were quite different from those during ~~7~~6-10 June, particularly those with endpoints at 500 m (Figs. 12a and 12c). About a half of the trajectories during 1-6 June originated from or moved through the PBL over North India (Fig. 12a), while nearly none of the trajectories during ~~7~~6-10 June had an opportunity to pass through the PBL over North India (Fig. 12c). Most of the trajectories during ~~7~~6-10 June originated either from the free troposphere over western Asia and Indian subcontinent or from the PBL south of NMC. Forward trajectories were also calculated for air masses originated from matrices of locations in the domains west and south of the NMC site. Examples of forward trajectories matrices are shown in Figure S6 for trajectories starting at 0600 UTC 3 June 2012 and 08 UTC 8 June 2012. The trajectories clearly indicate that the NMC site was impacted by air masses from different areas before and after 6 June. Around 4-5 June 2012, NMC was mainly impacted by air masses from the SW-W sector (North India, North Pakistan, and Nepal). Around 9-10 June, however, NMC was mainly impacted by air masses from the S-SW sector (Bangladesh, Bhutan, etc.). These results are consistent with those from the backward trajectories in Fig. 12. The above analysis can explain the sudden decrease of the PAN level after 6 June 2012 on one hand, and on the other hand support the idea that the PAN episode observed during 1-6 June 2012 was mainly caused by plumes from North India, North Pakistan, and Nepal.

Although the TP is one of the cleanest regions of the world, transport of anthropogenic pollutants to this region deserves attention. Some recent studies have showed that air pollutants can be transported to the Himalayas or to the TP region through passes like river valleys from the surroundings (Cong et al., 2007; Cong et al., 2009; Bonasoni et al., 2010; Kopacz et al., 2011; Lüthi et al., 2015; Shen et al., 2015; Zhang et al., 2015). The main source regions are South and East Asia. During the South Asian monsoon, the TP is predominately influenced by air masses from the Indian subcontinent. Impacts of transported pollutants on atmospheric environment over the Himalayas and TP, particularly the climate and hydrological effects of deposition of black carbon and other substances on Himalayan glaciers, have caused concerns (Ramanathan et al., 2007; Ming et al., 2012; Zhao et al., 2013; Qu et al., 2014; Wang et al., 2015; Zhang et al., 2015).

So far, studies of pollutants transport to the TP and its effect have focused on aerosols (compositions and optical depth) and less attention has been paid to the transport of gaseous

pollutants. There has been no previous report about impacts of long-range transport of pollutants on tropospheric photochemistry over the central TP region. Our results show, for the first time, that long-range transport of polluted airmasses from North India and other South Asian areas can significantly enhance ambient level of PAN at NMC. Although we have no observational data of PAN from other sites in the TP, it is likely that the entire convergence zone in the central and western TP (Figs. 11 and S4) was more or less impacted by the pollutants from South Asia. This implies that photochemistry over a large area in the TP was probably disturbed for at least ten days in the cases shown in Figs. 11 and S4. PAN transported to the TP region may be thermally and/or photolytically decomposed to release NO_x, acting as a chemical source of atmospheric NO_x over the TP, a region with very little anthropogenic emission of NO_x. The impacts of the transport of PAN and other related species on tropospheric photochemistry over the TP need to be studied in the future.

3.6 PAN levels at different heights over the TP

In addition to this study, in-situ PAN measurements from the TP are only reported by Xue et al. (2011). As PAN is a key source of NOx in remote regions, its concentration and distribution are important for understanding the photochemistry over regions like the TP. Here we provide a collection of PAN data for the TP region.

Table 1 summarizes the PAN data available for the TP from in-situ observations, satellite and space shuttle observations, and model simulations. Based on our in-situ observations at NMC (4.7 km), we obtained an averaged PAN level of 0.36 ppb for 17-24 August 2011 and 0.44 ppb for 15 May - 13 July 2012. In-situ observations at WLG (3.8 km) found an average PAN level of 0.44 for the period from 22 July to 16 August 2006 (Xue et al., 2011). The limited in-situ observations in the surface layer do not show substantial spatial and temporal differences in average level of PAN. However, the PAN level did show significant increases in some cases with obvious transport impacts from the UTLS (e.g., 22 August 2011) and from South Asia (e.g., 1-6 June 2012).

Developments in remote sensing have made it possible to detect global PAN in the UTLS from the space. During 9-13 August 1997, observations using the CRyogenic Infrared Spectrometers and Telescopes for the Atmosphere (CRISTA) aboard the Space Shuttle showed PAN levels in the range of 0.1-0.2 ppb for 18 km over the TP (Ungermann et al., 2016). Based on the retrievals of satellite observations using the Michelson Interferometer for

Passive Atmospheric Sounding (MIPAS), the average PAN levels in March 2003 were in the ranges of 0.15-0.23 ppb for 234 hPa and 0.35-0.45 ppb for 333 hPa over the TP, and those in August 2003 in the ranges of 0.15-0.23 ppb for 185 hPa and 0.35-0.50 ppb for 278 hPa (Moore and Remedios, 2010).The PAN level at 12 km over TP was about 0.10-0.15 ppb in October 2007 (Wiegele et al., 2012), which is very close to the range (0.1-0.2 ppb) on 21 October 2003 (Glatthor et al., 2007). Results from the model simulations by Fischer et al. (2014) show~~ed~~ that the PAN level during June-August 2008 varied in the range of 0.3-0.5 ppb in the 2-6 km layer and 0.2-0.4 ppb in the 6-10 km layer over the TP. Another model simulation study (Fadnavis et al., 2014) obtained a PAN range of 0.15-0.2 ppb for the 6-10 km layer and for June-September 1995-2004.

The satellite measurements and simulation results listed in Table 1 indicate a general decrease of PAN level from the upper troposphere to the lower stratosphere, consistent with the vertical distribution of PAN in the UTLS (Pope et al., 2016). These data represent PAN levels averaged over larger scales for certain periods. In-situ measurements on the ground show~~ed~~ average PAN levels very close to 333 hPa (about 10 km) values. So far, there has been no observation of the vertical distribution of PAN in the middle and lower troposphere over the TP. Based the results from the case studies in sections 3.4 and 3.5, we believe the PAN level in middle and lower tropospheric air over the TP may be more variable and sometimes elevated by transport of plumes from anthropogenic and biomass burning emissions. The significance of the transport impact deserves systematic studies, which is out the scope of this work.

4 Conclusions

For the first time, we made simultaneous ground-based measurements of two photochemical products, PAN and O_3 at Nam Co, a remote site in the central Tibetan Plateau (TP) region. Our effective PAN data cover two summer periods, i.e., from 17- to 24 August 2011 and from 15 May to 13 July 2012. The average levels of PAN were 0.36 ppb (range: 0.11-0.76 ppb) and 0.44 ppb (range: 0.21-0.99 ppb) in the 2011 and 2012 periods, respectively. During the observation in 2012, the O_3 level varied from 27.9 ppb to 96.4 ppb, with an average of 60.0 ppb, very close to the summertime O_3 level found at Waliguan, a global baseline station at the northeastern edge of the TP.

PAN and O_3 showed profound and similar diurnal cycles, with valleys around 5:00 LT, steep rises in the early morning, and broader platforms of high values during 9:00-20:00 LT. Such

patterns of diurnal variations of both gases, particularly the sharp increases even before sunrise, cannot be attributed solely to local photochemistry. Our analysis suggests that the PBL evolution played a key role in shaping the diurnal patterns of both gases. PAN and O_3 in the shallow nocturnal PBL were significantly removed by their sinks, such as chemical reactions and dry deposition. In the early morning, the elevation of the PBL height caused downward mixing of upper air containing higher PAN and O_3, leading to steep rises of the concentrations of these gases. The downward mixing and photochemistry sustained the higher levels of PAN and O_3 in the daytime. However, there were day-to-day differences in the PBL evolution, which could cause large differences in the diurnal variations of PAN and O_3. We identified two groups of days with different meteorological conditions and different diurnal patterns of trace gases and meteorological parameters. Days in Group 1 were mainly distributed in the pre-monsoon period, with higher daytime height of PBL (about 3 km), lower humidity, and larger day-night variations of PAN and O_3. Days in Group 2 were mainly distributed in the monsoon period, with shallower daytime PBL (about 2 km), higher humidity, and much smaller day-night variations of PAN and O_3.

There were some cases with obvious rapid transport of air masses during our observations. We identified two cases of rapid downward transport of air masses from the UTLS. The observed maximum PAN levels during these two cases ranged from 0.5 ppb to 0.7 ppb. These PAN levels are higher than those retrieved from satellite measurements for the UTLS. Therefore, it is likely that the tropospheric PAN over the TP may be disturbed for short periods, which is not easily captured by satellite observation. In addition to vertical transport of PAN, we also identified a case of strong long-range transport of PAN plumes. During this case, relatively polluted air masses from the PBL over North India, North Pakistan, and Nepal were able to be transported over the western and central TP to NMC, causing a profound episode of PAN with maximum close to 1 ppb during 1-6 June 2012. In contrast, significantly lower PAN levels were observed when air masses originated from other areas. Although transport of aerosols from South and Southeast Asia and its impacts on atmospheric environment over Himalayas and the TP have been intensively studied in recent years, transport of gaseous pollutants and its impacts have received less attention. Our results show, for the first time, that polluted air masses from South Asia can significantly enhance the ambient level of PAN at NMC. The space scale and frequency of this phenomenon and its impacts on tropospheric photochemistry over the TP region remain to be studied in the future.

Data availability. The observational data analyzed in this paper can be made available for scientific purposes by contacting the corresponding author (xiaobin_xu@189.cn).

Competing interests. The authors declare that they have no conflict of interest.

Acknowledgements. The authors thank the staff of the Nam Co station and Xizang Meteorological Bureau for logistical support. This work was supported by the China Special Fund for Meteorological Research in the Public Interest (GYHY201106023), the Natural Science Foundation of China (No.41330422) and Basic Research Fund of CAMS (2011Z003 and 2013Z005).

References

Bonasoni, P., Laj, P., Marinoni, A., Sprenger, M., Angelini, F., Arduini, J., Bonafè, U., Calzolari, F., Colombo, T., Decesari, S., Di Biagio, C., di Sarra, A. G., Evangelisti, F., Duchi, R., Facchini, M. C., Fuzzi, S., Gobbi, G. P., Maione, M., Panday, A., Roccato, F., Sellegri, K., Venzac, H., Verza, G. P., Villani, P., Vuillermoz, E., and Cristofanelli, P.: Atmospheric Brown Clouds in the Himalayas: first two years of continuous observations at the Nepal Climate Observatory-Pyramid (5079 m), Atmos. Chem. Phys., 10, 7515-7531, 2010.

Boersma, K.F., Eskes, H.J., Dirksen, R. J., van der A, R. J., Veefkind, J. P., Stammes, P., Huijnen, V., Kleipool, Q. L., Sneep, M., Claas, J., Leitao, J., Richter, A., Zhou, Y., and Brunner, D.: An improved retrieval of tropospheric NO_2 columns from the Ozone Monitoring Instrument, Atmos. Meas. Tech. , 4, 1905-1928, 2011

Chen, B., Xu, X. D., Yang, S., and Zhao, T. L.: Climatological perspectives of air transport from atmospheric boundary layer to tropopause layer over Asian monsoon regions during boreal summer inferred from Lagrangian approach, Atmos. Chem. Phys., 12, 5827-5839, 10.5194/acp-12-5827-2012, 2012.

Chen, X., An, J. A., Su, Z., Torre, L., Kelder, H., Peet, J., Ma, Y., and Fu, R.: The Deep Atmospheric Boundary Layer and Its Significance to the Stratosphere and Troposphere Exchange over the Tibetan Plateau, PloS One, 8, e56909, 10.1371/journal.pone.005690, 2013.

Cong, Z. Y., Kang, S. C., Liu, X. D., and Wang, G. F.: Elemental composition of aerosol in the Nam Co region, Tibetan Plateau, during summer monsoon season, Atmos. Environ., 41, 1180–1187, 2007.

Cong, Z. Y., Kang, S., Smirnov, A., and Holben, B.: Aerosol optical properties at Nam Co, a remote site in central Tibetan Plateau, Atmos. Res., 92, 42–48, 2009.

Cox, R.A. and Roffey, M.J.: Thermal decomposition of peroxyacetylnitrate in the presence of nitric oxide. Environ. Sci. & Technol., 11(9), 900–906,1977.

Cristofanelli, P., Bracci, A., Sprenger, M., Marinoni, A., Bonafè, U., Calzolari, F., Duchi, R., Laj, P., Pichon, J. M., Roccato, F., Venzac, H., Vuillermoz, E., and Bonasoni, P.: Tropospheric ozone variations at the Nepal Climate Observatory-Pyramid (Himalayas, 5079m a.s.l.) and influence of deep stratospheric intrusion events, Atmos. Chem. Phys., 10, 6537–6549, 2010.

De Smedt, I., Van Roozendael, M., Stavrakou, T., Müller, J.-F., Lerot, C. , Theys, N., Valks, P., Hao, N., and van der, N.A.: Improved retrieval of global tropospheric formaldehyde columns from GOME-2/MetOp-A addressing noise reduction and instrumental degradation issues. Atmos. Meas. Tech., 5, 2933-2949, 2012.

De Smedt, I., Müller, J.-F., Stavrakou, T., van der, A., R. J., Eskes, H. J., and Van Roozendael, M.: Twelve years of global observations of formaldehyde in the troposphere using GOME and SCIAMACHY sensors, Atmos. Chem. Phys., 8(16), 4947-4963, 2008.

Dessler, A. E., and Sherwood, S. C.: Effect of convection on the summertime extratropical lower stratosphere, J. Geophys. Res., 109, D23301-D23310, 10.1029/2004jd005209, 2004.

Ding, A. and Wang, T.: Influence of stratosphere-to-troposphere exchange on the seasonal cycle of surface ozone at Mount Waliguan in western China, Geophys. Res. Lett., 33, L03803, doi:10.1029/2005GL024760, 2006.

Draxler, R.R. and Hess, G.D.: Description of the HYSPLIT 4 modeling system. NOAA Technical Memorandum. ERLARL–224, NOAA Air Resources Laboratory, Silver Spring, MD. 24, 1997.

Fadnavis, S., Schultz, M.G., Semeniuk, K., Mahajan, A.S., Pozzoli, L., Sonbawne, S., Ghude, S.D., Kiefer, M., and Eckert, E.: Trends in peroxyacetyl nitrate (PAN) in the upper troposphere and lower stratosphere over southern Asia during the summer monsoon season: regional impacts, Atmos. Chem. Phys., 14, 12725–12743, 2014.

Fischer, E. V., Jaffe, D. A., Reidmiller, D. R., and Jaegle, L.: Meteorological controls on observed peroxyacetyl nitrate at Mount Bachelor during the spring of 2008, J. Geophys. Res., 115, D03302, doi:10.1029/2009jd012776, 2010.

Fischer, E. V., Jaffe, D. A., and Weatherhead, E. C.: Free tropospheric peroxyacetyl nitrate (PAN) and ozone at Mount Bachelor: potential causes of variability and timescale for trend detection, Atmos. Chem. Phys., 11, 5641-5654, 10.5194/acp-11-5641-2011, 2011.

Fischer, E. V., Jacob, D. J., Yantosca, R. M., Sulprizio, M. P., Millet, D. B., Mao, J., Paulot, F., Singh, H. B., Roiger, A. E., Ries, L., Talbot, R. W., Dzepina, K., and Pandey Deolal, S.: Atmospheric peroxyacetyl nitrate (PAN): a global budget and source attribution, Atmos. Chem. Phys., 14, 2679-2698, 2014.

Fishman, J., Wozniak,A.E., and Creilson, J.K.: Global distribution of tropospheric ozone from satellite measurements using the empirically corrected tropospheric ozone residual technique: Identification of the regional aspects of air pollution, Atmos. Chem. Phys., 3, 893–907, 2003.

Flocke, F.M., Weinheimer, A.J., Swanson, A.L., Roberts, J.M., Schmitt, R., and Shertz, S.: On the measurement of PANs by gas chromatography and electron capture detection, J. Atmos. Chem., 52, 19-43, 2005.

Ford, K. M., Campbell, B. M., Shepson, P. B., Bertman, S. B., Honrath, R. E., Peterson, M., and Dibb, J. E.: Studies of Peroxyacetyl nitrate (PAN) and its interaction with the snowpack at Summit, Greenland, J. Geophys. Res., 107, 4102-4111, 2002.

Fu, R., Hu, Y., Wright, J. S., Jiang, J. H., Dickinson, R. E., Chen, M., Filipiak, M., Read, W. G., Waters, J. W., Wu, D. L., and Affiliations, A.: Short circuit of water vapor and polluted air to the global stratosphere by convective transport over the Tibetan Plateau, PNAS, 103, 5664-5669, 10.1073/pnas.0601584103, 2006.

Gettelman, A., and Kinnison, D. E.: Impact of monsoon circulations on the upper troposphere and lower stratosphere, J. Geophys. Res., 109, D22101-D22114, 10.1029/2004jd004878, 2004.

Ghude, S.D., Jain, S.L., Arya, B.C., Beig, G., Ahammed, Y.N., Kumar, A., Tyagi, B.: Ozone in ambient air at a tropical megacity, Delhi: characteristics, trends and cumulative ozone exposure indices, J. Atmos. Chem., 60, 237–252, 2008.

Glatthor, N., von Clarmann, T., Fischer, H., Funke, B., Grabowski, U., Hopfner, M., Kellmann, S., Kiefer, M., Linden, A., Milz, M., Steck, T., and Stiller, G. P.: Global peroxyacetyl nitrate (PAN) retrieval in the upper troposphere from limb emission spectra of the Michelson Interferometer for Passive Atmospheric Sounding (MIPAS), Atmos. Chem. Phys., 7, 2775–2787, doi:10.5194/acp-7-2775-2007, 2007.

Gu, Y., Liao, H., and Bian, J.: Summertime nitrate aerosol in the upper troposphere and lower stratosphere over the Tibetan Plateau and the South Asian summer monsoon region, Atmos. Chem. Phys., 16, 6641-6663, doi:10.5194/acp-16-6641-2016, 2016.

Helmig, D., Oltmans, S. J., Morse, T. O., and Dibb, J. E.: What is causing high ozone at Summit, Greenland?, Atmos. Environ., 41, 5031-5043, doi:10.1016/j.atmosenv.2006.05.084, 2007.

Huang, Y., Wu, S., Kramer, L. J., Helmig, D., and Honrath, R. E.: Surface ozone and its precursors at Summit, Greenland: comparison between observations and model simulations, Atmos. Chem. Phys., 17, 14661-14674, https://doi.org/10.5194/acp-17-14661-2017, 2017.

Hudman, R.C., Jacob, D.J., Cooper, O.R., Evans, M.J., Heald, C.L., Park, R.J., Fehsenfeld, F., Flocke, F., Holloway, J., Hübler, G., Kita, K., Koike, M., Kondo, Y., Neuman, A., Nowak, J., Oltmans, S., Parrish, D., Roberts, J.M., and Ryerson, T.: Ozone production in transpacific Asian pollution plumes and implications for ozone air quality in California, J. Geophys. Res., 109, D23S10-D23S23, 10.1029/2004jd004974, 2004.

Kopacz, M., Mauzerall, D. L., Wang, J., Leibensperger, E. M., Henze, D. K., and Singh, K.: Origin and radiative forcing of black carbon transported to the Himalayas and Tibetan Plateau, Atmos. Chem. Phys., 11, 2837-2852, 10.5194/acp-11-2837-2011, 2011.

Kramer, L. J., Helmig, D., Burkhart, J. F., Stohl, A., Oltmans, S., and Honrath, R. E.: Seasonal variability of atmospheric nitrogen oxides and non-methane hydrocarbons at the GEOSummit station, Greenland, Atmos. Chem. Phys., 15, 6827-6849, doi:10.5194/acp-15-6827-2015, 2015.

LaFranchi, B. W., Wolfe, G. M., Thornton, J. A., Harrold, S. A., Browne, E. C., Min, K. E., Wooldridge, P. J., Gilman, J. B., Kuster, W. C., Goldan, P. D., de Gouw, J. A., McKay, M., Goldstein, A. H., Ren, X., Mao, J., and Cohen, R. C.,Closing the peroxy acetyl nitrate budget: observations of acyl peroxy nitrates (PAN, PPN, and MPAN) during BEARPEX 2007, Atmos. Chem. Phys., 9(19), 7623–7641, 2009.

Law, K. S.,Fierli, F., Cairo, F., Schlager, H., Borrmann, S., Streibel, M., Real, E., Kunkel, D., Schiller, C., Ravegnani, F., Ulanovsky, A., D'Amato, F., Viciani, S., Volk, C.M.: Air mass origins influencing TTL chemical composition over West Africa during 2006 summer monsoon, Atmos. Chem. Phys., 10, 10753–10770, 2010.

Lelieveld, J., Brühl, C., Jöckel, P., Steil, B., Crutzen, P. J., Fischer, H., Giorgetta, M. A., Hoor, P., Lawrence, M. G., Sausen, R., and Tost, H.: Stratospheric dryness: model simulations and satellite observations, Atmos. Chem. Phys., 7, 1313-1332, 2007.

Lelieveld, J. and Dentener, F. J.: What controls tropospheric ozone? J. Geophys. Res., 105(D3), 3531–3551, 2000.

Lefohn, A. S., Wernli, H., Shadwick, D., Oltmans, S. J., and Shapiro, M.: Quantifying the importance of stratospheric-tropospheric transport on surface ozone concentrations at high- and low-elevation monitoring sites in the United States, Atmos. Environ., 62, 646-656, 2012.

Li, M., Y. Ma, W. Ma, H. Ishiakawa, F. Sun, S. Ogino, Structural difference of atmospheric boundary layer between dry and rainy seasons over the central Tibetan Plateau (in Chinese),Journal of Glaciology and Geocryology, 33, 72-79, 2011.

Lin, W., Xu, X., Zheng, X., Jaxi, D., Ciren, B., Two-year measurements of surface ozone at Dangxiong, a remote highland site in the Tibetan Plateau, J. Environ. Sci., 31, 133-145, 2015.

Lüthi, Z.L., Škerlak, B., Kim, S.-W., Lauer, A., Mues, A., Rupakheti, M., and Kang, S.: Atmospheric Brown Clouds reach the Tibetan Plateau by crossing the Himalayas, Atmos. Chem. Phys., 15, 6007-6021, 2015.

Ma, J., Liu, H., and Hauglustaine, D.: Summertime tropospheric ozone over China simulated with a regional chemical transport model 1. Model description and evaluation, J. Geophys. Res., 107, ACH 27-21–ACH 27-13, doi:10.1029/2001JD001354, 2002a.

Ma, J., Tang, J., Zhou, X., and Zhang, X.: Estimates of the Chemical Budget for Ozone at Waliguan Observatory, J. Atmos. Chem., 41, 21–48, doi:10.1023/A:1013892308983, 2002b.

Ma, J., Lin, W. L., Zheng, X.D., Xu, X.B., Li, Z., and Yang, L.L.: Influence of air mass downward transport on the variability of surface ozone at Xianggelila Regional Atmosphere Background Station, southwest China, Atmos. Chem. Phys., 14, 5311–5325, 2014.

Ma, Y., Fan, S., Ishikawa, H., Tsukamoto, O., Yao, T., Koike, T., Zuo, H., Hu, Z., and Su, Z.: Diurnal and inter-monthly variation of land surface heat fluxes over the central Tibetan Plateau area, Theoret. Appl. Climat., 80, 259-273, 2005.

Ma, W., Ma, Y., and Bob, S.: Feasibility of Retrieving Land Surface Heat Fluxes from ASTER Data Using SEBS: a Case Study from the NamCo Area of the Tibetan Plateau, Arctic, Antarctic, and Alpine Research, 43(2), 239-245, 2011.

Ming, J., Du, Z., Xiao, C., Xu, X., and Zhang, D.: Darkening of the mid-Himalaya glaciers since 2000 and the potential causes, Environ. Res. Lett. 7, 014021, doi:10.1088/1748-9326/7/1/014021, 2012.

Moore, D.P. and Remedios, J.J.: Seasonality of Peroxyacetyl nitrate (PAN) in the upper troposphere and lower stratosphere using the MIPAS-E instrument, Atmos. Chem. Phys., 10, 6117-6128, 10.5194/acp-10-6117-2010, 2010.

Myhre, G., Shindell, D., Bréon, F.-M., Collins, W., Fuglestvedt, J., Huang, J., Koch, D., Lamarque, J.-F., Lee, D., Mendoza, B., Nakajima, T., Robock, A., Stephens, G., Takemura, T., and Zhang, H.: Anthropogenic and Natural Radiative Forcing. In: Climate Change 2013: The Physical Science Basis. Contribution of Working Group I to the Fifth Assessment Report of the Intergovernmental Panel on Climate Change [Stocker, T.F., D. Qin, G.-K. Plattner, M. Tignor, S.K. Allen, J. Boschung, A. Nauels, Y. Xia, V. Bex and P.M. Midgley (eds.)]. Cambridge University Press, Cambridge, United Kingdom and New York, NY, USA, 2013.

Ohara,T., Akimoto, H., Kurokawa, J., Horii, N., Yamaji, k., Yan, X., and Hayasaka, T.: An Asian emission inventory of anthropogenic emission sources for the period 1980–2020, Atmos. Chem. Phys., 7, 4419–4444, 2007.

Pandey Deolal, S., Staehelin, J., Brunner, D., Cui, J., Steinbacher, M., Zellweger, C., Henne, S., and Vollmer, M. K.: Transport of PAN and NOy from different source regions to the Swiss high alpine site Jungfraujoch, Atmos. Envron., 64, 103–115, doi:10.1016/j.atmosenv.2012.08.021, 2013.

Park, M., Randel, W. J., Gettelman, A., Massie, S. T., and Jiang, J. H.: Transport above the Asian summer monsoon anticyclone inferred from Aura Microwave Limb Sounder tracers, J. Geophys. Res., 112, 10.1029/2006jd008294, 2007.

Park, M., Randel, W. J., Emmons, L. K., Bernath, P. F., Walker, K. A., and Boone, C. D.: Chemical isolation in the Asian monsoon anticyclone observed in Atmospheric Chemistry Experiment (ACE-FTS) data, Atmos. Chem. Phys., 8, 757-764, 10.5194/acp-8-757-2008, 2008.

Park, M., Randel, W. J., Emmons, L. K., and Livesey, N. J.: Transport pathways of carbon monoxide in the Asian summer monsoon diagnosed from Model of Ozone and Related Tracers (MOZART), J. Geophys. Res., 114, D08303-D08313, 10.1029/2008jd010621, 2009.

Pope, R. J., Richards, N. A. D., Chipperfield, M. P., Moore, D. P., Monks, S. A., Arnold, S. R., Glatthor, N., Kiefer, M., Breider, T. J., Harrison, J. J., Remedios, J. J., Warneke, C., Roberts, J. M., Diskin, G. S., Huey, L. G., Wisthaler, A., Apel, E. C., Bernath, P. F., and Feng, W.: Intercomparison and evaluation of satellite peroxyacetyl nitrate observations in the upper

troposphere–lower stratosphere, Atmos. Chem. Phys., 16, 13541-13559, https://doi.org/10.5194/acp-16-13541-2016, 2016.

Qu, B., Ming, J., Kang, S.-C., Zhang, G.-S., Li, Y.-W., Li, C.-D., Zhao, S.-Y., Ji, Z.-M., and Cao, J.-J.: The decreasing albedo of the Zhadang glacier on western Nyainqentanglha and the role of light-absorbing impurities, Atmos. Chem. Phys., 14, 11117-11128, doi:10.5194/acp-14-11117-2014, 2014.

Ramanathan, V., Ramana, M. V., Roberts, G., Kim, D., Corrigan, C., Chung, C., Winker, D.: Warming trends in Asia amplified by brown clouds solar absorption, Nature, 448, 575–578, 2007.

Ran, L., Lin, W.L., Deji, Y.Z., La, B., Tsering, P.M., Xu, X.B., and Wang, W.: Surface gas pollutants in Lhasa, a highland city of Tibet: current levels and pollution implications, Atmos. Chem. Phys. 14, 10721–10730, 2014.

Randel, W. J., Park, M., Emmons, L., Kinnison, D., Bernath, P., Walker, K. A., Boone, C., and Pumphrey, H.: Asian Monsoon Transport of Pollution to the Stratosphere, Science Magazine, 328, 611-613, 10.1126/science.1182274, 2010.

Remedios, J. J., Allen, G., Waterfall, A. M., Oelhaf, H., Kleinert, A., and Moore1, D. P.: Detection of organic compound signatures in infra-red, limb emission spectra observed by the MIPAS-B2 balloon instrument, Atmos. Chem. Phys., 7, 1599-1613, 10.5194/acp-7-1599-2007, 2007.

Roiger, A., Aufmhoff, H., Stock, P., Arnold, F., and Schlager, H.: An aircraft-borne chemical ionization - ion trap mass spectrometer (CI-ITMS) for fast PAN and PPN measurements, Atmos. Meas. Tech., 4, 173-188, 10.5194/amt-4-173-2011, 2011.

Roberts, J. M.: PAN and Related Compounds, in: Volatile Organic Compounds in the Atmosphere, edited by: Koppmann,R., Blackwell Publishing, 500, Oxford, UK, 2007.

Russo, R. S., Talbot, R. W., Dibb, J. E., Scheuer, E., Seid, G., Jordan, C. E., Fuelberg, H. E., Sachse, G. W., Avery, M. A., Vay, S. A., Blake, D. R., Blake, N. J., Atlas, E., Fried, A., Sandholm, S. T., Tan, D., Singh, H. B., Snow, J., and Heikes, B. G.: Chemical composition of Asian continental outflow over the western Pacific: Results from Transport and Chemical Evolution over the Pacific (TRACE-P), J. Geophys. Res., 108, 10.1029/2002jd003184, 2003.

Shen, R.-Q., Ding, X., He, Q.-F., Cong, Z.-Y., Yu, Q.-Q., and Wang, X.M.: Seasonal variation of secondary organic aerosol tracers in Central Tibetan Plateau, Atmos. Chem. Phys., 15, 8781-8793, 2015.

Singh, H.B.: Reactive nitrogen in the troposphere. Environ. Sci. & Technol., 21(4), 320–327, 1987.

Singh, H.B., Salas, L., Herlth, D., Kolyer, R., Czech, E., Avery, M., Crawford, J.H., Pierce, R.B., Sachse, G.W., Blake, D.R., Cohen, R. C., Bertram, T.H., Perring, A., Wooldridge, P.J., Dibb, J., Huey, G., Hudman, R.C., Turquety, S., Emmons, L.K., Flocke, F., Tang, Y., Carmichael, G.R., and Horowitz, L.W.: Reactive nitrogen distribution and partitioning in the North American troposphere and lowermost stratosphere, J. Geophys. Res., 112, D12S04, doi:10.1029/2006JD007664, 2007.

Sudo, K., Takahashi, M., and Akimoto, H.: CHASER: A global chemical model of the troposphere 2. Model results and evaluation, J. Geophys. Res, 107, 4586, doi:10.1029/2001jd001114, 2002.

Stull, R.B.: An Introduction to Boundary Layer Meteorology, Kluwer Academic, Dordrecht, The Netherlands, 1988.

Talbot, R. W., Dibb, J. E., Scheuer, E. M., Kondo, Y., Koike, M., Singh, H. B., Salas, L. B., Fukui, Y., Ballenthin, J. O., Meads, R. F., Miller, T. M., Hunton, D. E., Viggiano, A. A., Blake, D. R., Blake, N. J., Atlas, E., Flocke, F., Jacob, D. J., and Jaegle, L.: Reactive nitrogen budget during the NASA SONEX Mission, Geophys. Res. Lett., 26, 3057-3060, 10.1029/1999GL900589, 1999.

Talukdar, R. K., Burkholder, J. B., Schmoltner, A.-M., Roberts, J. M., Wilson, R. R., and Ravishankara, A. R.: Investigation of the loss processes for peroxyacetyl nitrate in the atmosphere: UV photolysis and reaction with OH, J. Geophys. Res., 100, 14163–14173, 10.1029/95JD00545, 1995.

Thakur, A.N., Singh, H.B., Mariani, P., Chen, Y., Wang, Y., Jacob, D.J., Brasseur, G., Müller, J.F., and Lawrence, M.: Distribution of reactive nitrogen species in the remote free troposphere: data and model comparisons, Atmos. Environ., 33, 1403–1422, doi:10.1016/s1352-2310(98)00281-7, 1999.

Tereszchuk, K.A., Moore, D.P., Harrison, J.J., Boone, C.D., Park, M., Remedios, J.J., Randel, W.J., and Bernath, P.F.: Observations of peroxyacetyl nitrate (PAN) in the upper troposphere

by the Atmospheric Chemistry Experiment-Fourier Transform Spectrometer (ACE-FTS), Atmos. Chem. Phys., 13, 5601-5613, 10.5194/acp-13-5601-2013, 2013.

Tian, W., Chipperfield, M., and Huang, Q.: Effects of the Tibetan Plateau on total column ozone distribution, Tellus B, 60, 622-635, 10.1111/j.1600-0889.2008.00338.x, 2008.

Ungermann, J., Ern, M., Kaufmann, M., Müller, R., Spang, R., Ploeger, F., Vogel, B., and Riese, M.: Observations of PAN and its confinement in the Asian summer monsoon anticyclone in high spatial resolution, Atmos. Chem. Phys., 16, 8389–8403, 2016.

Volz-Thomas, A., Xueref, I., and Schmitt, R.: An automatic gas chromatograph and calibration system for ambient measureme, Environ. Sci. Pollut. Res., 9, 72-76, 2002.

von Kuhlmann, R., Lawrence, M.G., Crutzen, P.J., and Rasch, P.J.: A model for studies of tropospheric ozone and nonmethane hydrocarbons: Model evaluation of ozone-related species, J. Geophys. Res, 108, 4729, doi:10.1029/2002jd003348, 2003.

Wang, M., Xu, B., Cao, J., Tie, X., Wang, H., Zhang, R., Qian, Y., Rasch, P. J., Zhao, S., Wu, G., Zhao, H., Joswiak, D. R., Li, J., and Xie, Y.: Carbonaceous aerosols recorded in a southeastern Tibetan glacier: analysis of temporal variations and model estimates of sources and radiative forcing, Atmos. Chem. Phys., 15, 1191-1204, doi:10.5194/acp-15-1191-2015, 2015.

Wang, T., Wong, H.L.A., Tang, J., Ding, A., Wu, W.S., and Zhang, X.C.: On the origin of surface ozone and reactive nitrogen observed at a remote mountain site in the northeastern Qinghai-Tibetan Plateau, western China, J. Geophys. Res., 111, D08303, doi:10.1029/2005JD006527, 2006.

Wang, Q.Y., Gao, R.S., Cao, J.J., Schwarz, J.P., Fahey, D.W., Shen, Z.X., Hu, T.F., Wang, P., Xu, X.B., and Huang, R.J.: Observations of high level of ozone at Qinghai Lake basin in the northeastern Qinghai-Tibetan Plateau, western China, J. Atmos. Chem., 72, 19–26, 2015.

Wiegele, A., Glatthor, N., Höpfner, M., Grabowski, U., Kellmann, S., Linden, A., Stiller, G., and von Clarmann, T.: Global distributions of C_2H_6, C_2H_2, HCN, and PAN retrieved from MIPAS reduced spectral resolution measurements, Atmos. Meas. Tech., 5, 723-734, 10.5194/amt-5-723-2012, 2012.

Worden, J., Jones, D.B.A., Liu, J., Parrington, M., Bowman, K., Stajner, I., Beer, R., Jiang, J., Thouret, V., Kulawik, S., Li, J.-L. F., Verma, S., and Worden, H.: Observed vertical

distribution of tropospheric ozone during the Asian summertime monsoon, J. Geophys. Res., 114, D13304-D13320, 10.1029/2008jd010560, 2009.

Xiong, X., Houweling, S., Wei, J., Maddy, E., Sun, F., and Barnet, C.: Methane plume over south Asia during the monsoon season: satellite observation and model simulation, Atmos. Chem. Phys., 9, 783-794, 2009.

Xu, W., Lin, W., Xu, X., Tang, J., Huang, J., Wu, H., and Zhang, X., Long-term trends of surface ozone and its influencing factors at the Mt. Waliguan GAW station, China – Part 1: Overall trends and characteristics, Atmos. Chem. Phys., 16, 6191–6205, 2016.

Xu, W., Xu, X., Lin, M., Lin, W., Tarasick, D., Tang, J., Ma, J., and Zheng, X.: Long-term trends of surface ozone and its influencing factors at the Mt. Waliguan GAW station, China - Part 2: The roles of anthropogenic emissions and climate variability, Atmos. Chem. Phys., 18, 773-798, https://doi.org/10.5194/acp-2017-483, 2018.

Xue, L.K., Wang, T., Zhang, J.M., Zhang, X.C., Deliger, Poon, C.N., Ding, A.J., Zhou, X.H., Wu, W.S., Tang, J., Zhang, Q.Z., and Wang, W.X.: Source of surface ozone and reactive nitrogen speciation at Mount Waliguan in western China: New insights from the 2006 summer study, J. Geophys. Res., 116, 10.1029/2010jd014735, 2011.

Yeh, T.-C., Lo, S.-W., and Chu, P.-C.: The wind structure and heat balance in the lower troposphere over Tibetan Plateau and its surroundings, Acta Meteor. Sinica (in Chinese), 28, 108-121, 1957.

Yin, X., Kang, S., de Foy, B., Cong, Z., Luo, J., Zhang, L., Ma, Y., Zhang, G., Rupakheti, D., and Zhang, Q.: Surface ozone at Nam Co (4730 m a.s.l.) in the inland Tibetan Plateau: variation, synthesis comparison and regional representativeness, Atmos. Chem. Phys. Discuss., https://doi.org/10.5194/acp-2017-175, 2017.

Zanis, P., Ganser, A., Zellweger, C., Henne, S., Steinbacher, M., and Staehelin, J.: Seasonal variability of measured ozone production efficiencies in the lower free troposphere of Central Europe, Atmos. Chem. Phys., 7, 223-236, 10.5194/acp-7-223-2007, 2007.

Zellweger, C., Ammann, M., Buchmann, B., Hofer, P., Lugauer, M., Rüttimann, R., Streit, N., Weingartner, E., and Baltensperger, U.: Summertime NO_y Speciation at the Jungfraujoch, 3580 m asl, Switzerland, J. Geophys. Res., 105, 6655–6667, 2000.

Zellweger, C., Klausen, J., Buchmann, B., and Scheel, H.-E.: System and Performance Audit of Surface Ozone, Carbon Monoxide, Methane and Nitrous Oxide at the GAW Global Station Mt. Waliguan and the Chinese Academy of Meteorological Sciences (CAMS) China, June 2009, WCC-Empa Report 09/2Rep., 61 pp, Empa, Dübendorf, Switzerland, available at: https://www.wmo.int/pages/prog/arep/gaw/documents/WLG_2009.pdf (last access: 15 January 2018), 2009.

Zhang, H., Xu, X., Lin, W., and Wang, Y.: Wintertime peroxyacetyl nitrate (PAN) in the megacity Beijing: Role of photochemical and meteorological processes, J. Environ. Sci., 26, 83–96, 10.1016/S1001-0742(13)60384-8, 2014.

Zhang, J.M., Wang, T., Ding, A.J., Zhou, X.H., Xue, L.K., Poon, C.N., Wu, W.S., Gao, J., Zuo, H.C., Chen, J.M., Zhang, X.C., and Fan, S.J.: Continuous measurement of peroxyacetyl nitrate (PAN) in suburban and remote areas of western China, Atmos. Environ., 43, 228-237, 2009a.

Zhang, L., Jacob, D.J., Boersma, K.F., Jaffe, D.A., Olson, J.R., Bowman, K.W., Worden, J.R., Thompson, A.M., Avery, M.A., Cohen, R.C., Dibb, J.E., Flock, F.M., Fuelberg, H.E., Huey, L.G., McMillan, W.W., Singh, H.B., and Weinheimer, A.J.: Transpacific transport of ozone pollution and the effect of recent Asian emission increases on air quality in North America: an integrated analysis using satellite, aircraft, ozonesonde, and surface observations, Atmos. Chem. Phys., 8, 6117–6136, doi:10.5194/acp-8-6117-2008, 2008.

Zhang, Q., Streets, D.G., Carmichael, G.R., He, K.B., Huo, H., Kannari, A., Klimont, Z., Park, I.S., Reddy, S., Fu, J.S., Chen, D., Duan, L., Lei, Y., Wang, L.T., Yao, Z.L., Asian emissions in 2006 for the NASA INTEX-B mission, Atmos. Chem. Phys. 9, 5131-5153, 2009b .

Zhang, Q., Kang, S., and Zhang, G.: Changes of snow line altitude for glaciers on western Nyainqentanglha range observed by remote sensing, Scientia Geographica Sinica,36, 1937-1944, 2016.

Zhang, R., Wang, H., Qian, Y., Rasch, P. J., Easter, R. C., Ma, P.-L., Singh, B., Huang, J., and Fu, Q.: Quantifying sources, transport, deposition and radiative forcing of black carbon over the Himalayas and Tibetan Plateau, Atmos. Chem. Phys., 15, 6205–6223, 2015.

Zhao, S., Ming, J., Sun, J., and Xiao, C.: Observation of carbonaceous aerosols during 2006–2009 in Nyainqêntanglha Mountains and the implications for glaciers, Environ. Sci. Pollut. Res., DOI 10.1007/s11356-013-1548-6, 2013.

Zheng, X. D., Shen, C. D., Wan, G. J., Liu, K. X., Tang, J., and Xu, X. B.: $^{10}Be/^{7}Be$ implies the contribution of stratosphere-troposphere transport to the winter-spring surface O_3 variation observed on the Tibetan Plateau, Chinese Sci. Bull., 56, 84–88, 2011.

Zhou, X., Lou, C., Li, W.L. and Shi, J.E. Ozone changes over China and low center over Tibetan Plateau, Chin. Sci. Bull., 40, 1396–1398, 1995.

Zhu, L., Fischer, E.V., Payne, V.H., Worden, J.R., and Jiang, Z.: TES observations of the interannual variability of PAN over Northern Eurasia and the relationship to springtime fires, Geophys. Res. Lett., 42, 7230-7237, doi:10.1002/2015GL065328, 2015.

Zhu, T., Lin, W.L., Song, Y., Cai, X.H., Zou, H., Kang, L., Zhou, L.B., and Akimoto, H.: Downward transport of ozone-rich air near Mt. Everest, Geophys. Res. Lett. 33 (23), L23809, doi: 10.1029/2006GL027726, 2006.

1 Table 1 Measured and modeled PAN at different heights over the TP.

PAN (ppb)	Period	Height[a]	Method	Reference
0.35(0.11-0.76) [b]	17-24 August 2011	4.7 km	Ground measurements	this work
0.44(0.21-0.99) [b]	15 May - 13 July 2012	4.7 km	Ground measurements	
0.52(0.31-0.72)[b]	22 August 2011	4.7 km	Ground measurements with impact from the UT	
0.40(0.24-0.50)[b]	25 May 2012	4.7 km	Ground measurements with impact from the UT	
0.62(0.27-0.99) [b]	1-6 June 2012	4.7 km	Ground measurements with impact from South Asia	
0.44(0.14)[c]	22 July - 16 August 2006	3.8 km	Ground measurements	Xue et al.(2011)
0.35-0.45[d]	March 2003	333 hPa	MIPAS	Moore and Remedios (2010)
0.15-0.23[d]		234 hPa	MIPAS	
0.35-0.5[d]	August 2003	278 hPa	MIPAS	
0.15-0.23[d]		185 hPa	MIPAS	
0.1-0.15[d]	October 2007	12 km	MIPAS	Wiegele et al.(2012)
0.1-0.2[d]	21 October 2003	12 km	MIPAS	Glatthor et al.(2007)
0.1-0.2[d]	9-13 August 1997	18 km	Space Schuttle experiment	Ungermann et al.(2016)

			CRISTA-2	
0.3-0.5[d]	June-August 2008	2-6 km	GEOS-Chem modeling	Fischer et al.(2014)
0.2-0.4[d]		6-10 km	GEOS-Chem simulation	
0.15-0.2[d]	June-September 1995-2004	6-10 km	ECHAM5-HAMMOZ model simulation	Fadnavis et al.(2014)

[a] Either elevation above the sea level or air pressure layer.

[b] Overall average with the range of hourly mean.

[c] Overall average with standard deviation.

[d] Reading based on the color scale given in the reference.

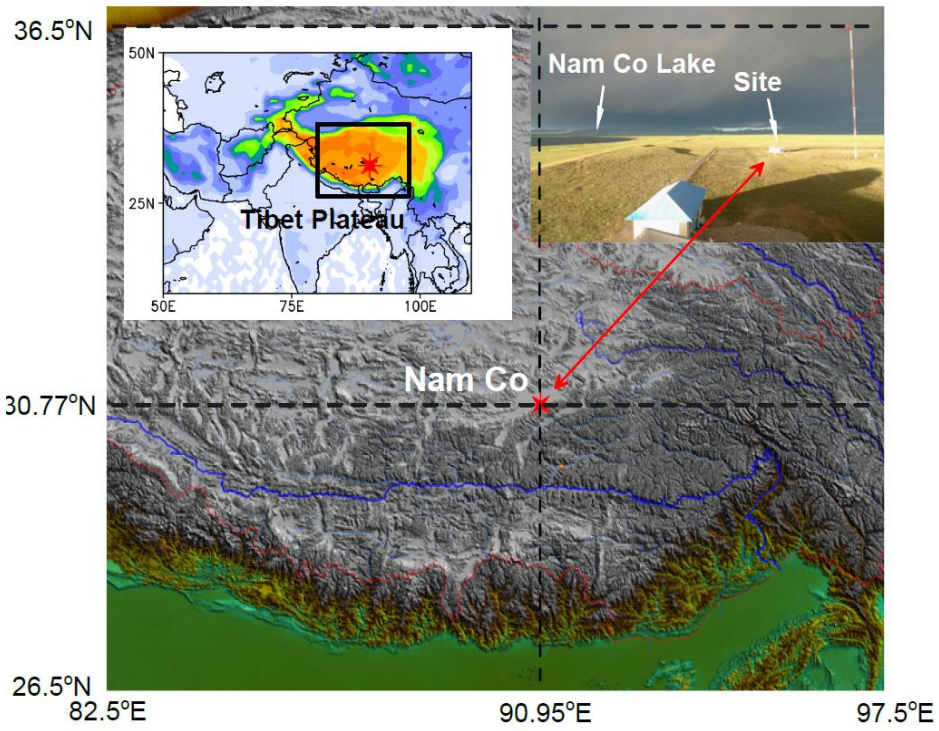

Fig.1 Map showing location of the observation site and local environment.

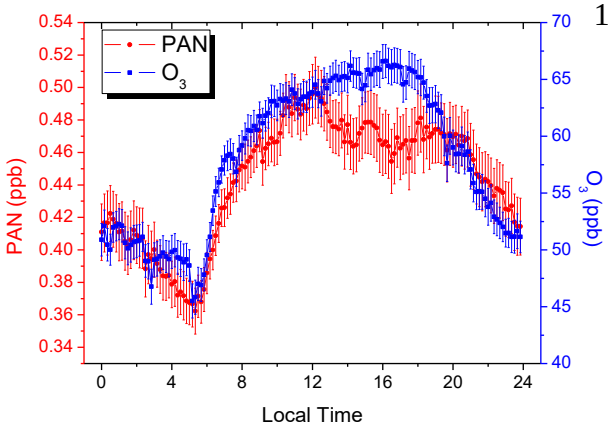

Fig.2 Diurnal patterns of PAN and O_3. All data are processed as 10 minutes resolution. The vertical bars represent one standard error of the mean.

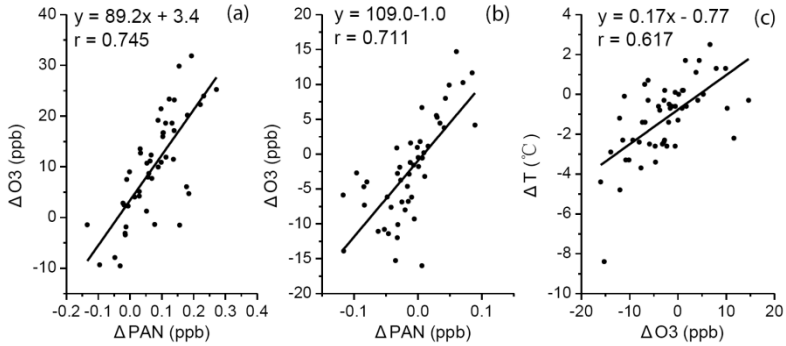

Fig.3 Scatter plots of ΔPAN (variation of the PAN concentration), ΔO_3 (variation of the O_3 concentration) and ΔT (variation of temperature) in specific time spans: (a) from 5:00 LT to 9:00 LT; (b, c) from 2:00 LT to 4:00 LT. All correlations shown in the figures are statistically significant at α=0.01.

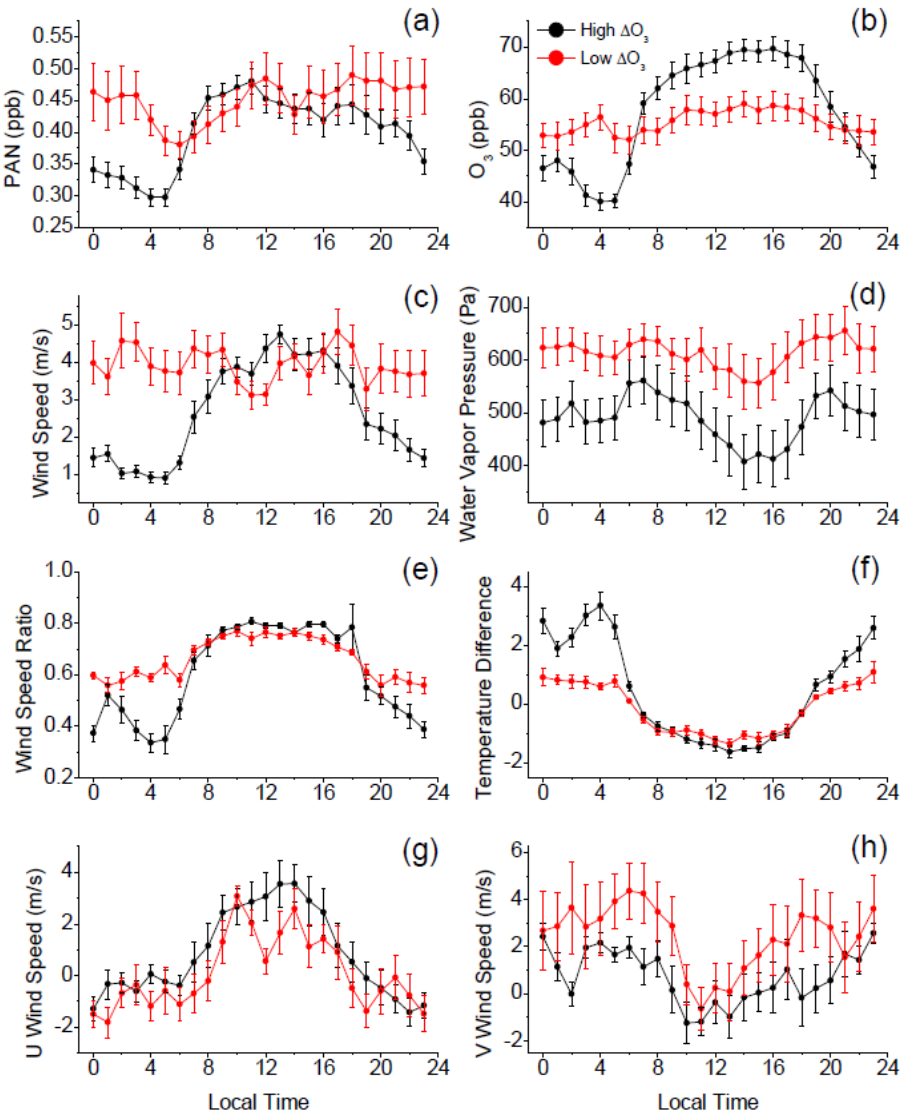

Fig. 4 Diurnal patterns of PAN (a), O_3 (b), ~~Wind~~ wind ~~Speed~~ speed (c), ~~Water~~ water ~~Vapor~~ vapor ~~Pressure~~ pressure (d), ~~Wind~~ wind ~~Speed~~ speed ~~Ratio~~ ratio (e, ratio of 10 meters height wind speed and 2 meters height wind speed), ~~Temperature~~ temperature ~~Difference~~ difference (f, subtraction of 20 meters height temperature and 10 meters height temperature), U wind speed (g) and V wind speed (h). Black curves represent diurnal curves of 15 days with greatest ΔO_3 from 7:00 LT to 11:00 LT, and red curves represent diurnal curves of 15 days with smallest ΔO_3 ~~correspondently~~. The vertical bars represent one standard error of the mean.

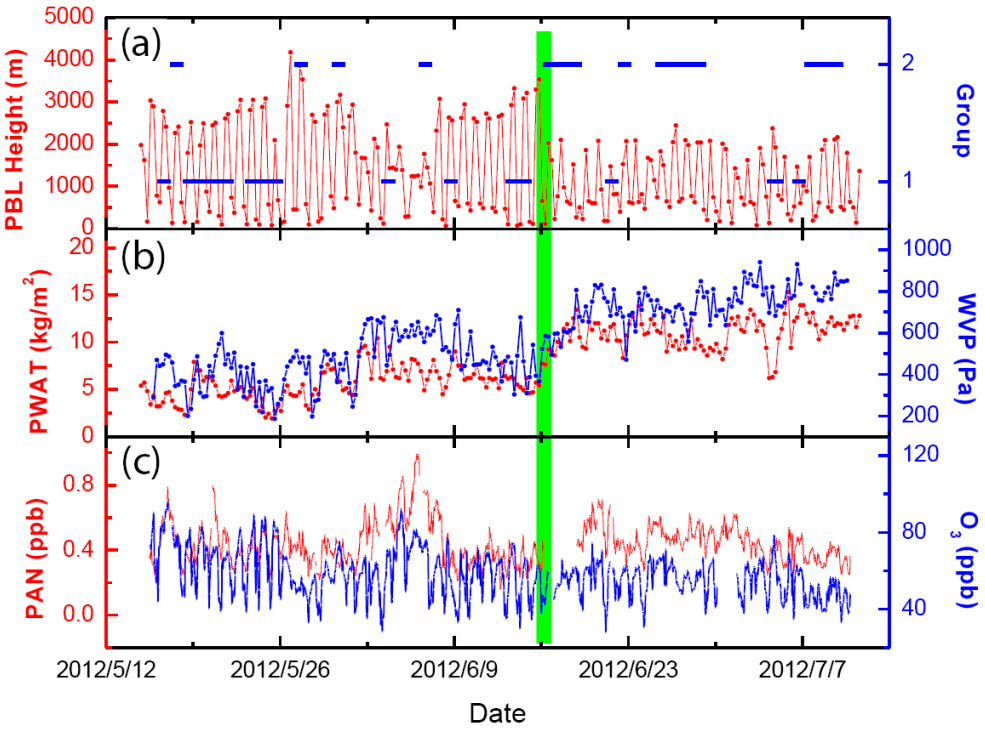

Fig. 5 Distributions of two groups of days and time series the PBL height, PWAT (~~Precipitable~~ precipitable ~~Water~~ water of ~~Entire~~ entire ~~Atmosphere~~atmosphere), WVP (~~Water~~ water ~~Vapor~~ vapor ~~Pressure~~pressure), PAN and O_3. Groups 1 and 2 represent two groups of days with different O_3 enhancement (ΔO_3) during 5:00-10:00 LT, with Group 1 including 15 days with the greatest ΔO_3 (denoted as High ΔO_3 in Fig. 4) and Group 2 including 15 days with the smallest ΔO_3 (denoted as Low ΔO_3 in Fig. 4). The PBL ~~Height~~ height and PWAT were acquired from the FNL data with temporal resolution of 6 hours. WVP were calculated and processed as 6-hours resolution data from field observation. PAN and O_3 concentrations were processed as hourly data.

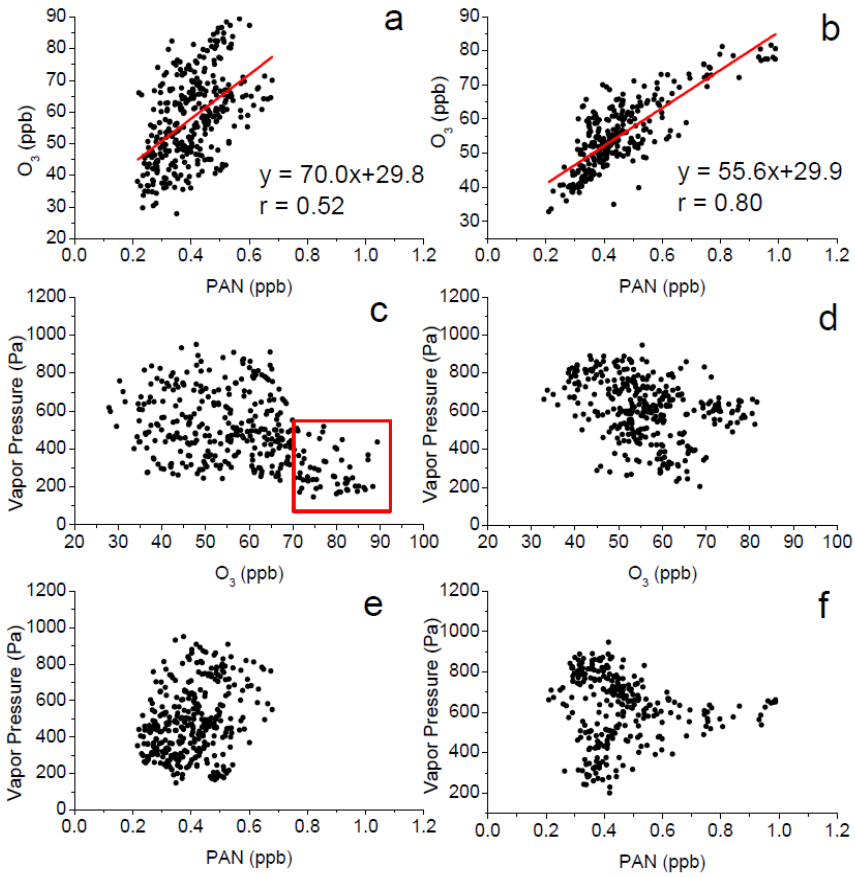

Fig. 6 Scatter plots of hourly O_3 versus PAN, ~~Vapor~~ vapor ~~Pressure~~ pressure versus O_3, ~~Vapor~~ vapor ~~Pressure~~ pressure versus PAN of group 1 (a,c,e) and group 2 (b,d,f), following Fig. 4. The correlation shown in Figs. 6(a) and 6(b) are significant at α=0.01. The data points within the red rectangle in Fig. 6(c) represent O_3 levels higher than 70 ppb and WVP lower than 500 Pa.

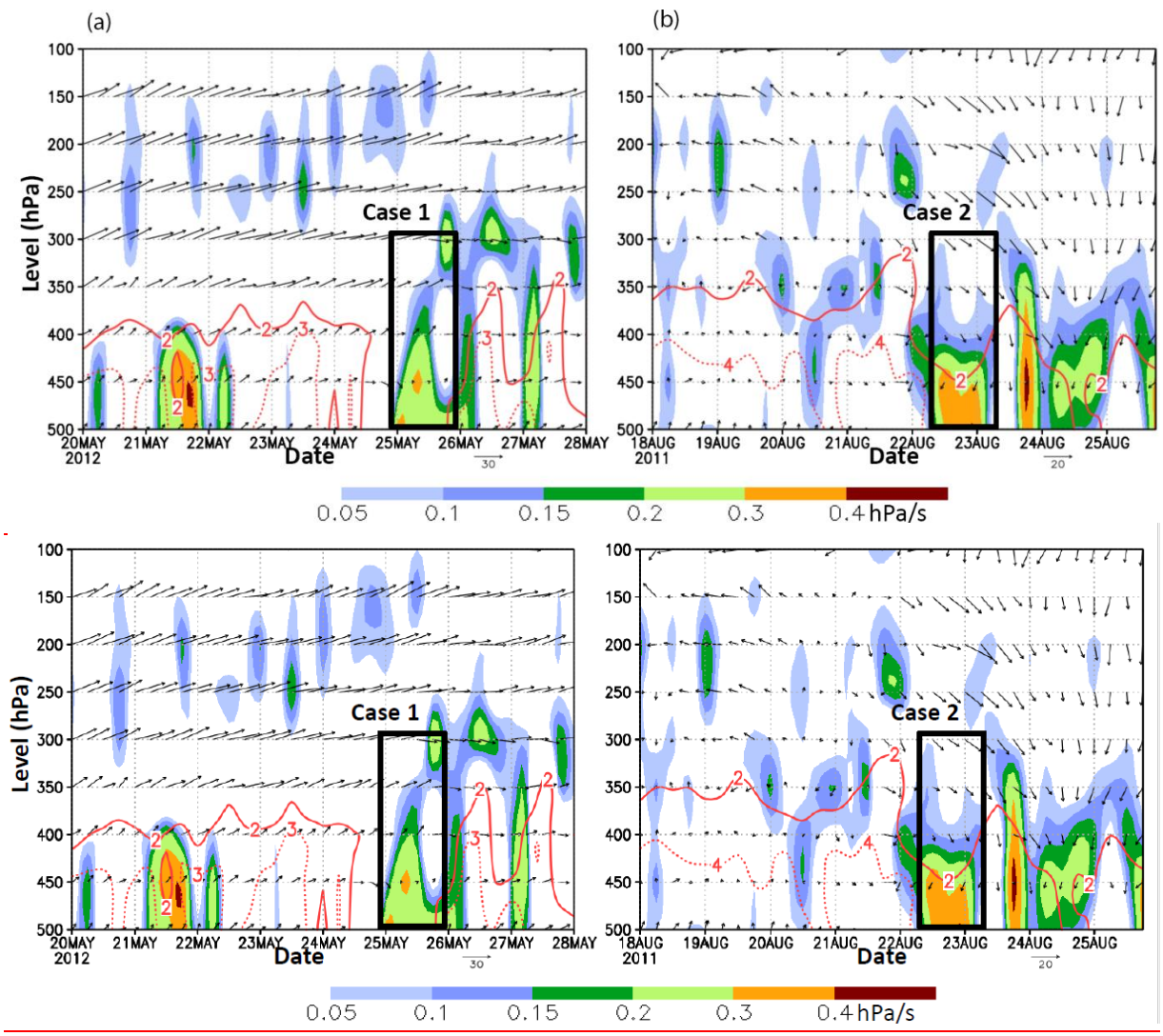

Fig. 7 Omega (shaded), specific humidity (red line) and horizontal wind field in dependence of time and height in two time frames. (a) From 20 to 28 May 2012; (b) From 18 to 25 August 2011. Case 1 and Case 2 correspond to two significant downdraft events.

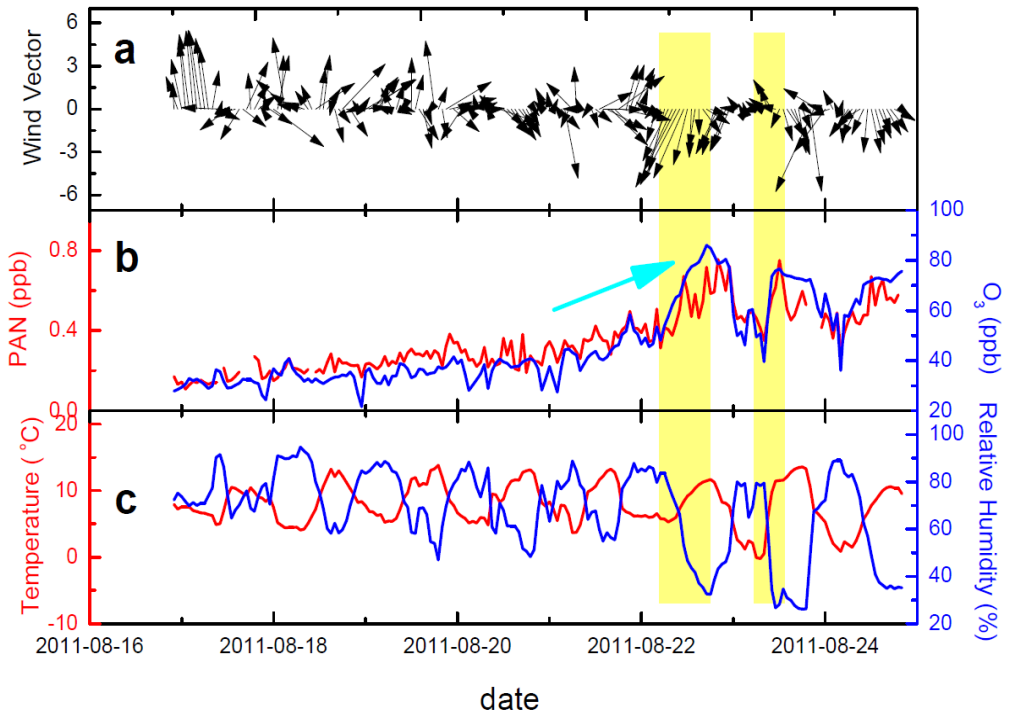

Fig. 8 Time series of (a) surface wind vectors, (b) PAN and O_3, and (c) temperature and relative humidity during 17-24 August 2011. Yellow shadows represent the short periods controlled by downward motion. The blue arrow indicates the increasing trend of PAN and O_3.

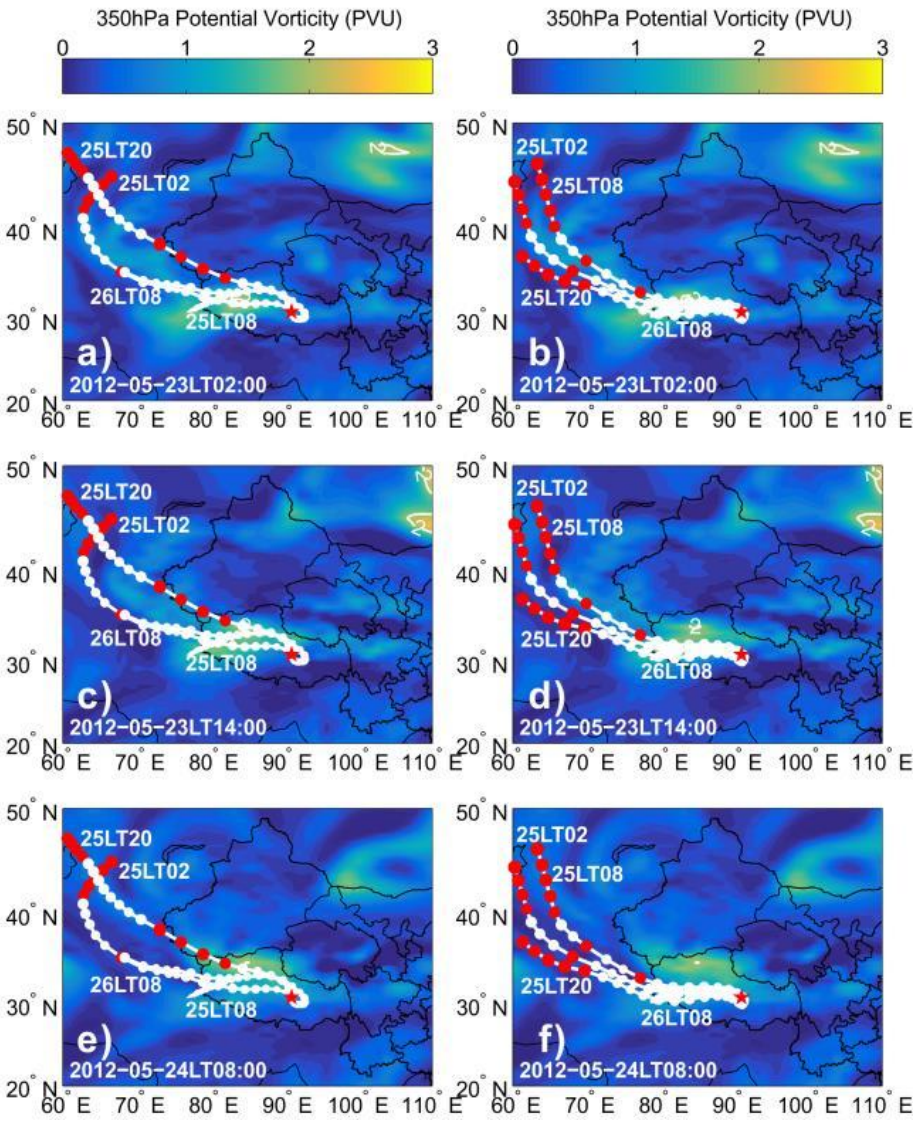

Fig. 9 ~~Plots showing~~ The 350 hPa potential vorticity fields at three time-points during 23-24 May 2012 and back trajectories of air masses arriving at 500 m (a,c,e) and 1500 m (b,d,f) above the ground of NMC (red star) during 25-26 May 2012.

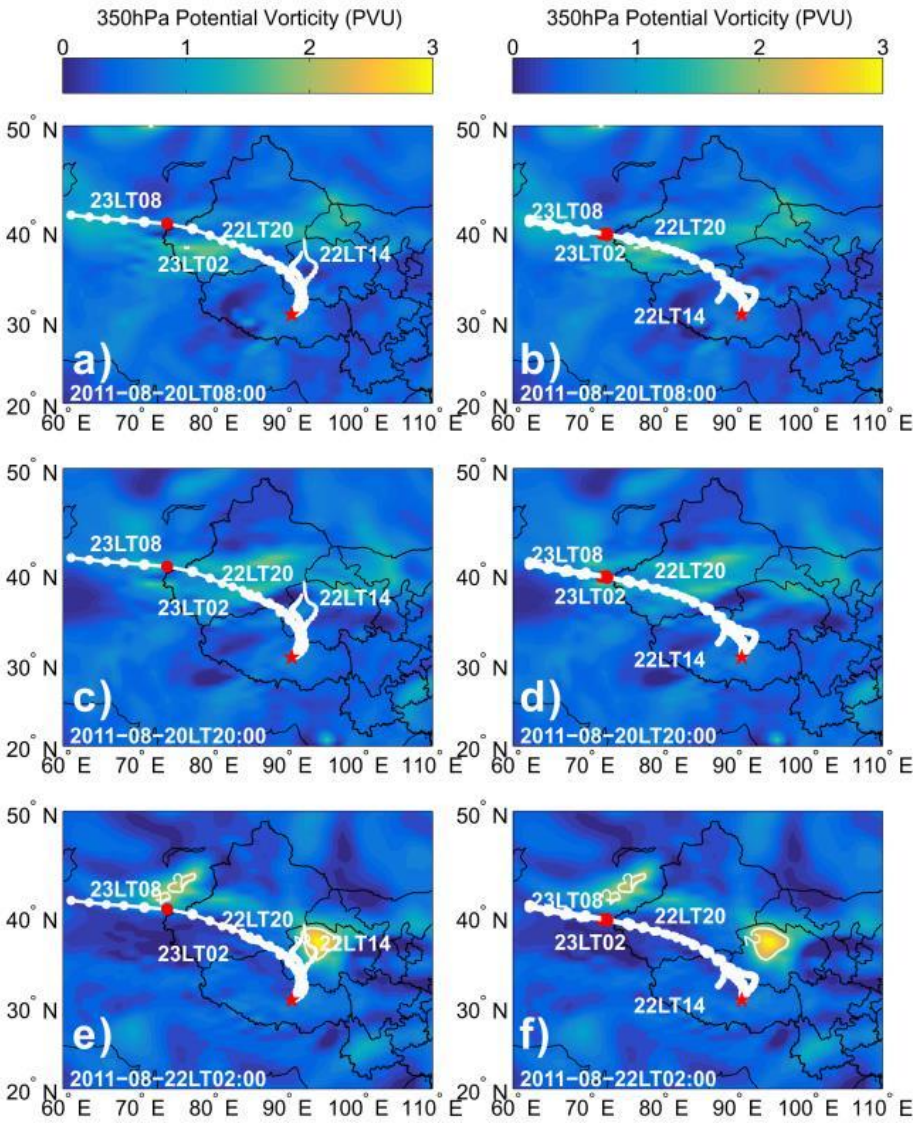

Fig. 10 Same as Fig. 9, but for 22-23 August 2011.

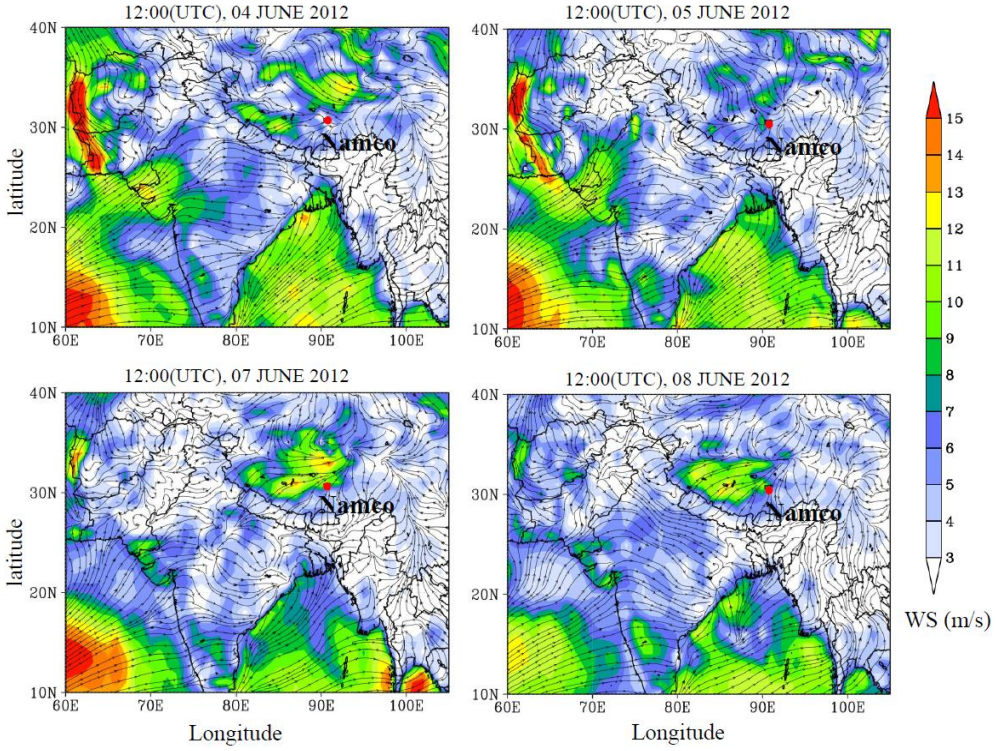

Fig. 11 Average fields of wind at sigma=0.995 for 12:00 (UTC) of 4, 5, 7 and 8 June 2012.

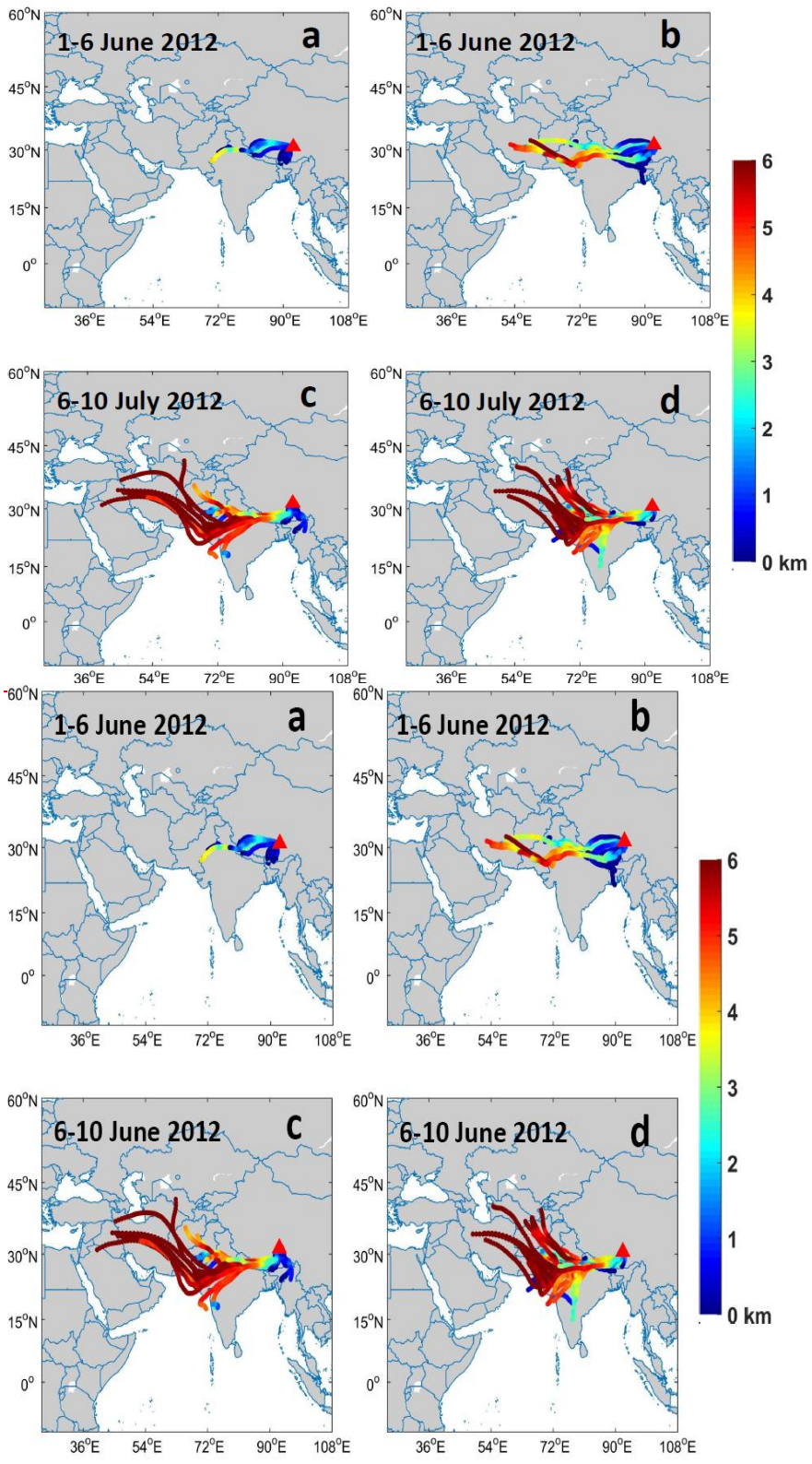

Fig. 12 Backward air trajectories arriving at NMC with endpoint heights of 500 meters (a,c) 1500 meters (b,d) for the periods 1-6 June 2012 (a,b) and ~~7~~6-10 June 2012 (c,d). The color scale shows trajectory heights in km above ground level.

Supplementary Materials for

First simultaneous measurements of peroxyacetyl nitrate (PAN) and ozone at Nam Co in the central Tibetan Plateau: impacts from the PBL evolution and transport processes

Xiaobin Xu[1], Hualong Zhang[1,*], Weili Lin[1,2,], Ying Wang[1], Wanyun Xu[1], and Shihui Jia[1,**]**

[1] State Key Laboratory of Severe Weather & Key Laboratory for Atmospheric Chemistry of China Meteorological Administration, Chinese Academy of Meteorological Sciences, Beijing, China

[2] Meteorological Observation Center, China Meteorological Administration, Beijing, China

[*] now at : Guangdong Meteorological Observatory, Guangzhou, Guangdong, China

[**] now at: College of Life and Environmental Sciences, Minzu University of China, Beijing, China

[***] now at: School of Environment and Energy, South China University of Technology, Guangzhou, Guangdong, China

Correspondence to: Xiaobin Xu (xiaobin_xu@189.cn)

Indirect calibration of PAN measurements

To obtain acceptable results using the indirect calibration method, we need two assumptions. First, the ambient concentration of CCl_4 at the observation site should be nearly constant during the measurement period. Second, whatever the ECD sensitivity changes with varying environmental conditions, the changes in relative responses of the ECD to PAN and CCl_4 should be the same during the period of consideration. In polluted areas, the first assumption is inapplicable simply because there is large spatial and temporal variation of CCl_4 emission. Even at the regional background site often impacted by polluted air masses, the CCl_4 concentration could be highly varying (Yao et al., 2010). However, CCl_4 is believed to be well mixed to a large scale in clean area air due to negligible emission and long lifetime

(42 ±12 years), thus its concentration at remote sites can be treated as constant in a short period (Simmonds et al., 1998). Based on this idea, Wang et al. (2000) suggested using CCl_4 as an internal reference in the preparation of standard gas mixtures. The second assumption is prerequired for any application of similar indirect calibration and normally applicable if the ECD sensitivity is stable with a GC run. On the basis of the two assumptions above, the ratio between the PAN and CCl_4 signals is used as the key quantity for correcting the PAN data. Therefore, the corrected PAN concentration is eventually determined by following expression:

$$C'_{PAN} = (C_{PAN} \times S'_{PAN} \times S_{CCl4})/(S_{PAN} \times S'_{CCl4}) , \quad (1)$$

where, C'_{PAN} and C_{PAN} are the concentrations of ambient and standard PAN, respectively; S'_{PAN} and S_{PAN} are the PAN signals of air sample and standard sample, respectively; and S'_{CCl4} and S_{CCl4} are the CCl_4 signals of the air sample and the surrogate CCl_4 signal of the calibration, respectively. Since the standard sample did not contain CCl_4, the CCl_4 signal of the air sample prior to a calibration was taken as the surrogate of CCl_4 signal for the calibration run (S'_{CCl4}). This may introduce additional uncertainty to the PAN data as the ECD sensitivity may change from run to run. However, the change of the ECD sensitivity should be minor between consecutive runs within relative short time. Therefore, equation (1) is acceptable in our indirect calibration.

References

Simmonds, P. G., Cunnold, D. M., Weiss, R. F., Prinn, R. G., Fraser, P. J., McCulloch, A., Alyea, F. N., and O'Doherty, S.: Global trends and emission estimates of CCl_4 from in situ background observations from July 1978 to June 1996, J. Geophys. Res., 103, 16017–16027, 10.1029/98JD01022, 1998.

Wang, J.-L., Lin, W.-C., and Chen, T.-Y.: Using atmospheric CCl_4 as an internal reference in gas standard preparation, Atmos. Environ., 34, 4393–4398, 2000.

Yao, B., Zhou, L.X., Zhang, F., Xu, L., Zang, K.P., Zhang, X.C., Zhang, X.L., Zhou, H.G., Dong, F., and Zhou, L.Y.: In-situ measurement of atmospheric carbon tetrachloride (CCl_4) at the Shangdianzi Global Atmosphere Watch regional station, Acta Scientiae Circumstantiae, 30(12), 2377-2382, 2010.

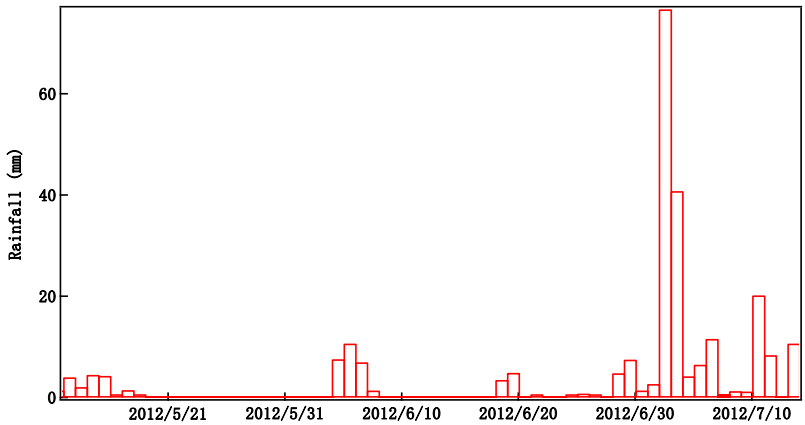

Figure S1 Daily rainfall during the observation period in 2012.

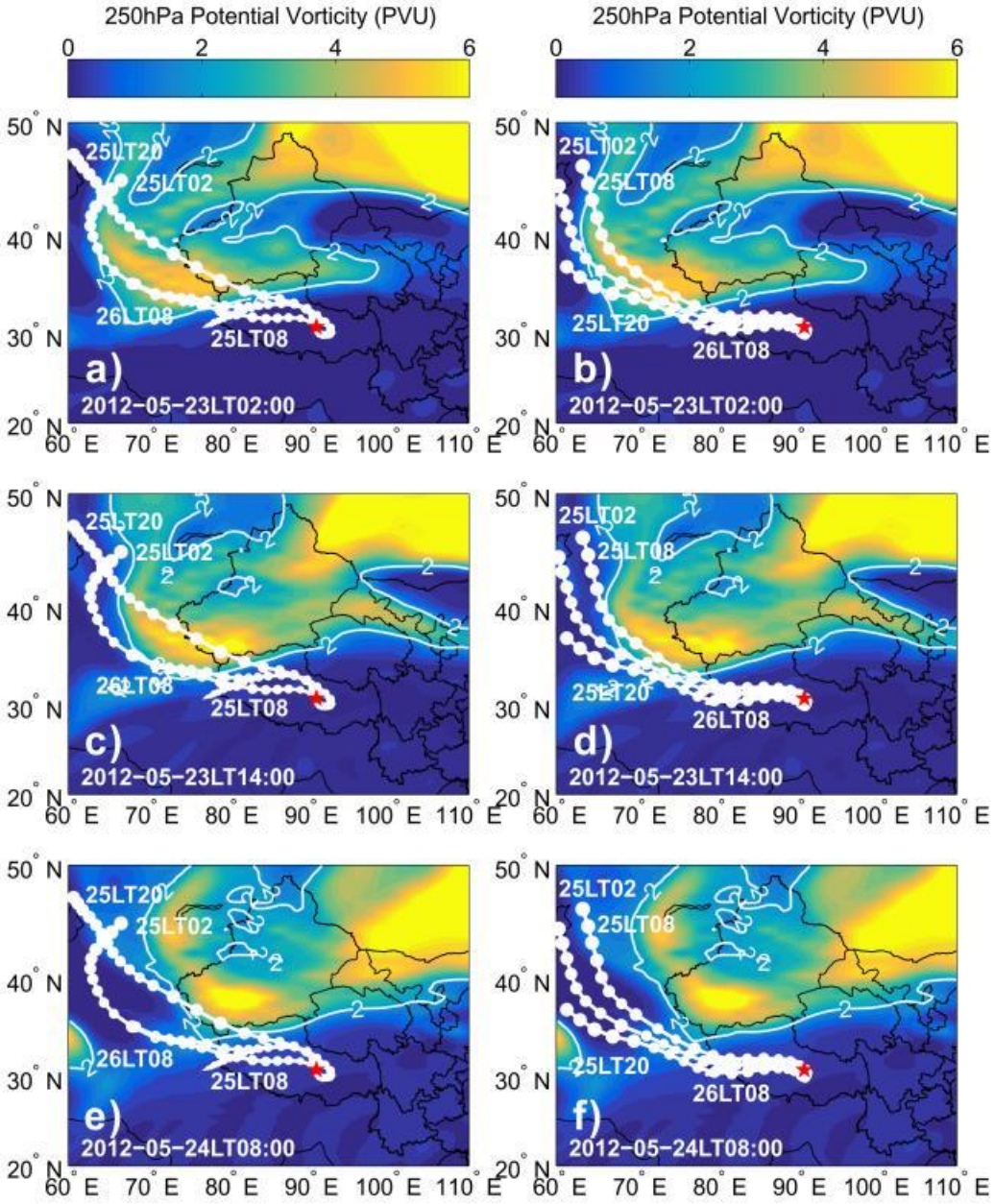

Figure S2 ~~Plots showing~~The 250 hPa potential vorticity fields at three timepoints during 23-24 May 2012 and back trajectories of air masses arriving at 500 m (left) and 1500 m (right) above ground of the NMC site (red star) during 25-26 May 2012.

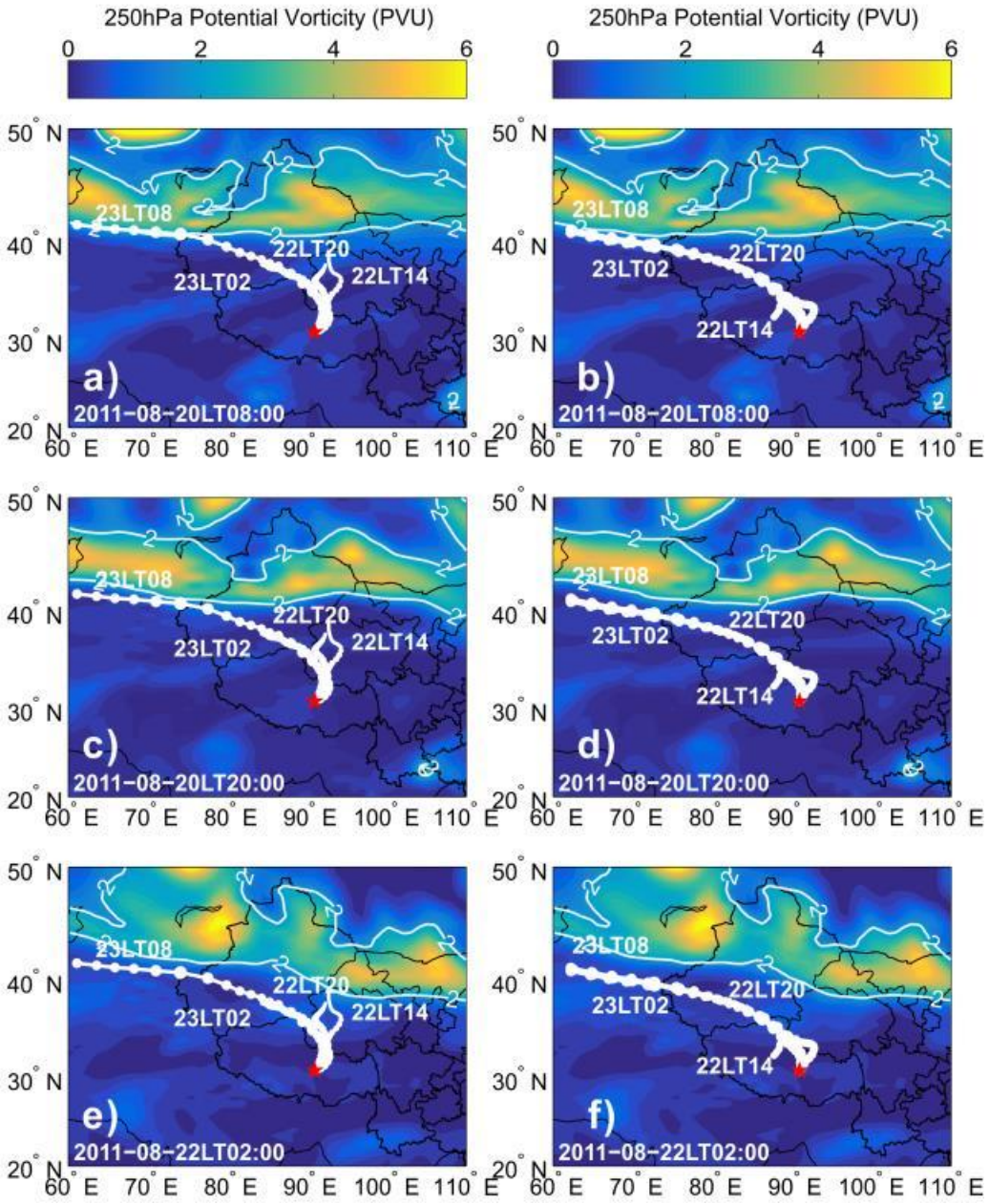

Figure S3 Same Figure S2, but for 22-23 August 2011.

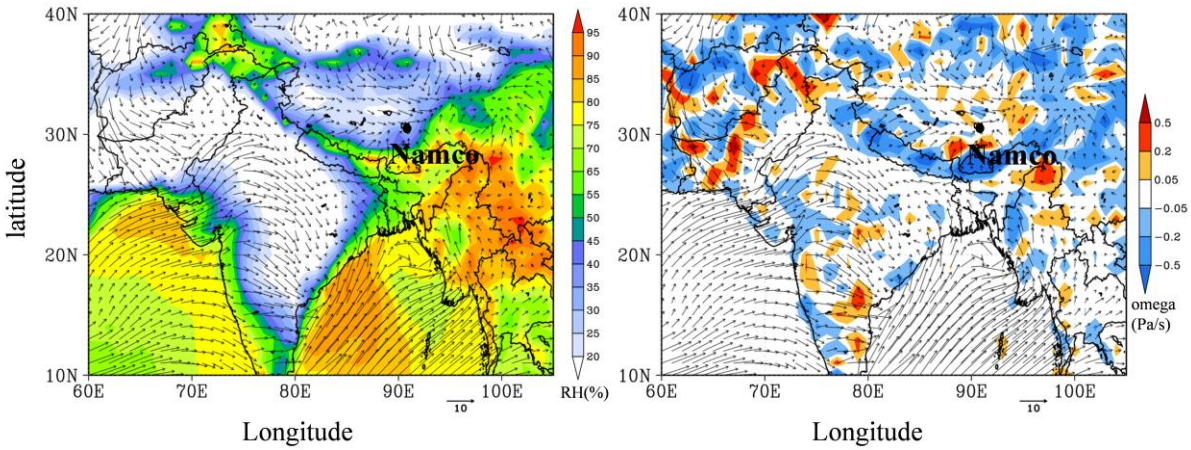

Figure S4 Average fields of wind, relative humidity (a) and omega (b) at sigma=0.995 for the periods 30-31 May 2012.

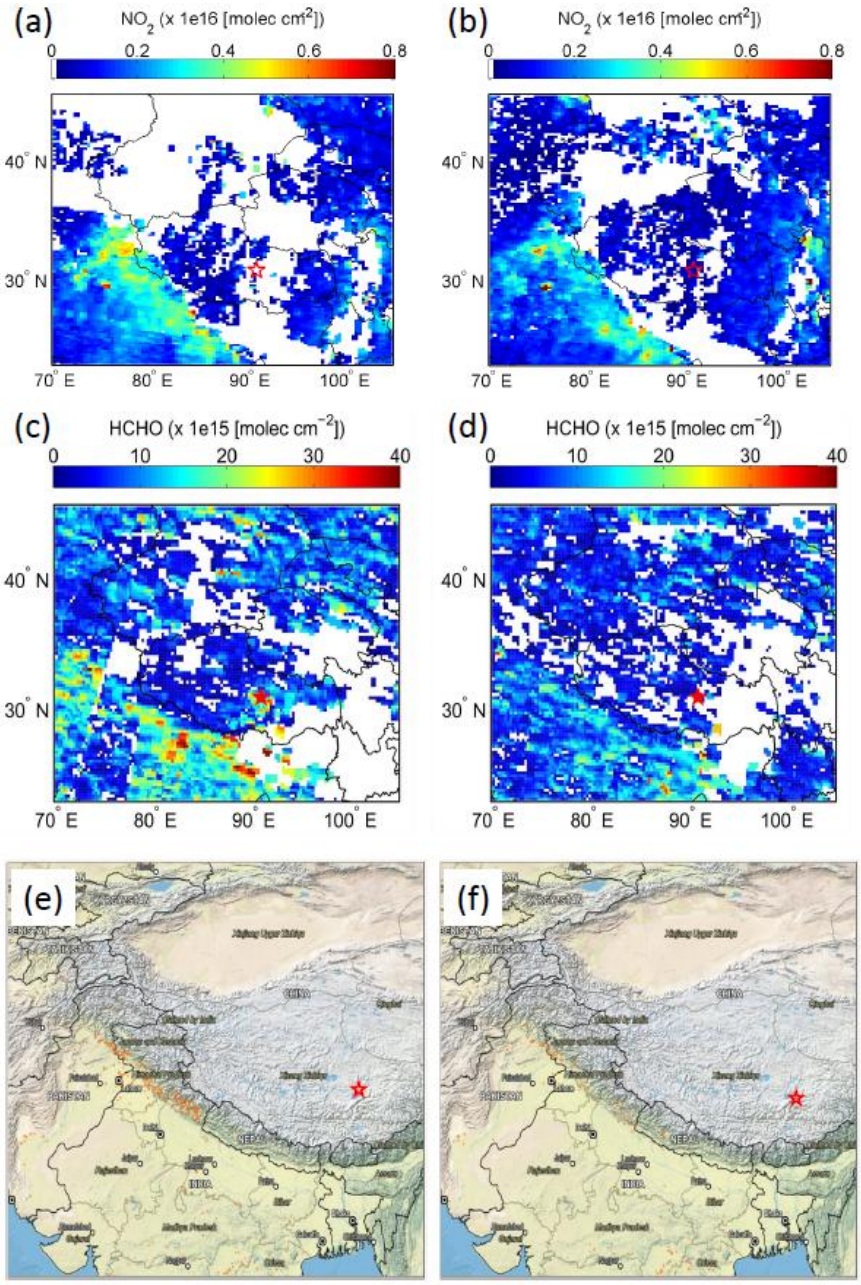

Figure S5 Average column densities of tropospheric NO_2 (a,b) and HCHO (c,d), and maps with fire spots (e,f) for the periods 1-3 (a,c,e) and 4-6 June 2012 (b,d,f). Daily tropospheric NO_2 data are from the OMI observations and made available by NASA (https://daac.gsfc.nasa.gov/datasets). Daily tropospheric HCHO are from GOME-2 observations and provided by the Tropospheric Emission Monitoring Internet Service (TEMIS) at The Royal Netherlands Meteorological Institute (KNMI), The Netherlands (http://www.temis.nl/index.php). Fire spots maps present the fire locations (orange dots) observed by MODIS and are produced by NASA's Web Fire Mapper (https://firms.modaps.eosdis.nasa.gov/firemap/).

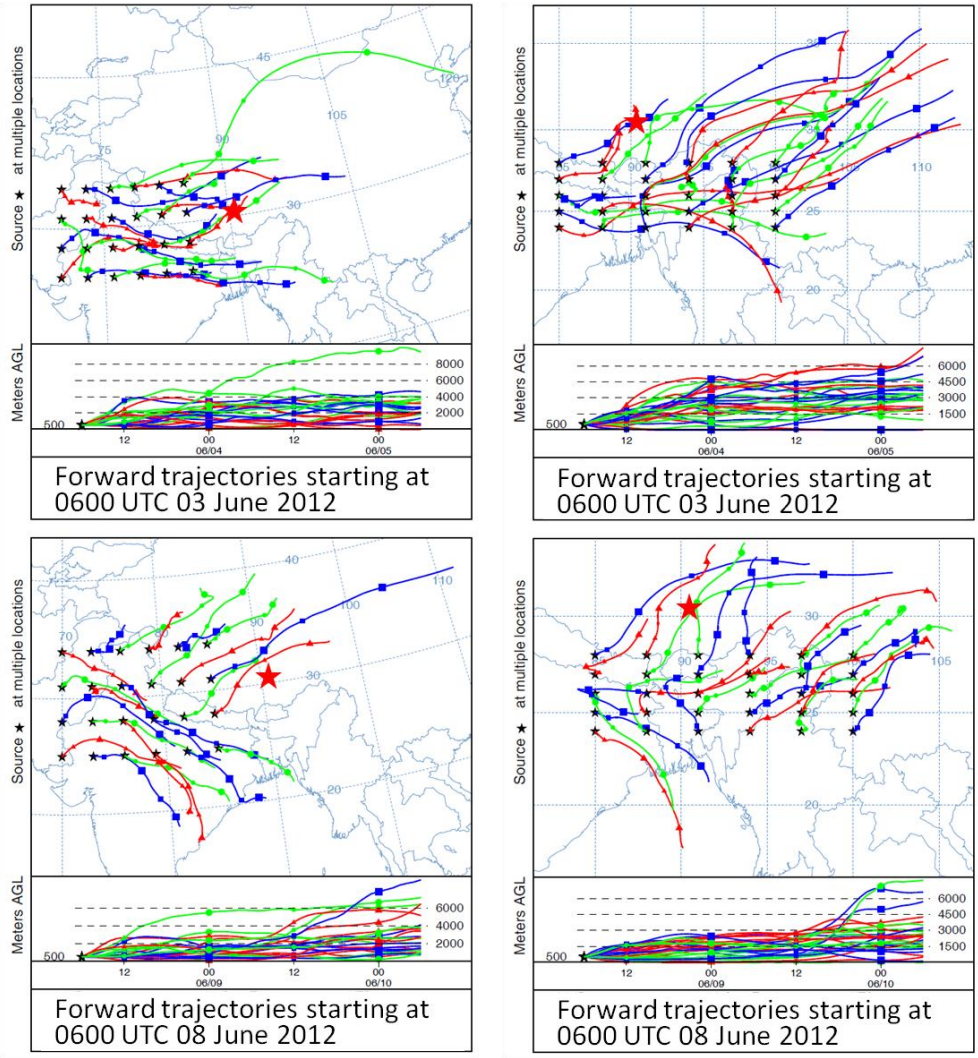

Figure S6 Matrices of 48-h air mass forward trajectories starting at 0600 UTC 3 June 2012 (upper panel) and 0600 UTC 8 June 2012 (bottom panel) from the domains west and south of the NMC site (red star). The online HYSPLIT model (https://ready.arl.noaa.gov/HYSPLIT_traj.php; Stein et al., 2015; Rolph et al., 2017) were used to produce the trajectory matrices. The starting height of the trajectories is 500 m above ground level.

Stein, A.F., Draxler, R.R, Rolph, G.D., Stunder, B.J.B., Cohen, M.D., and Ngan, F.: NOAA's HYSPLIT atmospheric transport and dispersion modeling system, Bull. Amer. Meteor. Soc., 96, 2059-2077, 2015.

Rolph, G., Stein, A., and Stunder, B.: Real-time Environmental Applications and Display system: READY. Environmental Modelling & Software, 95, 210-228, 2017.